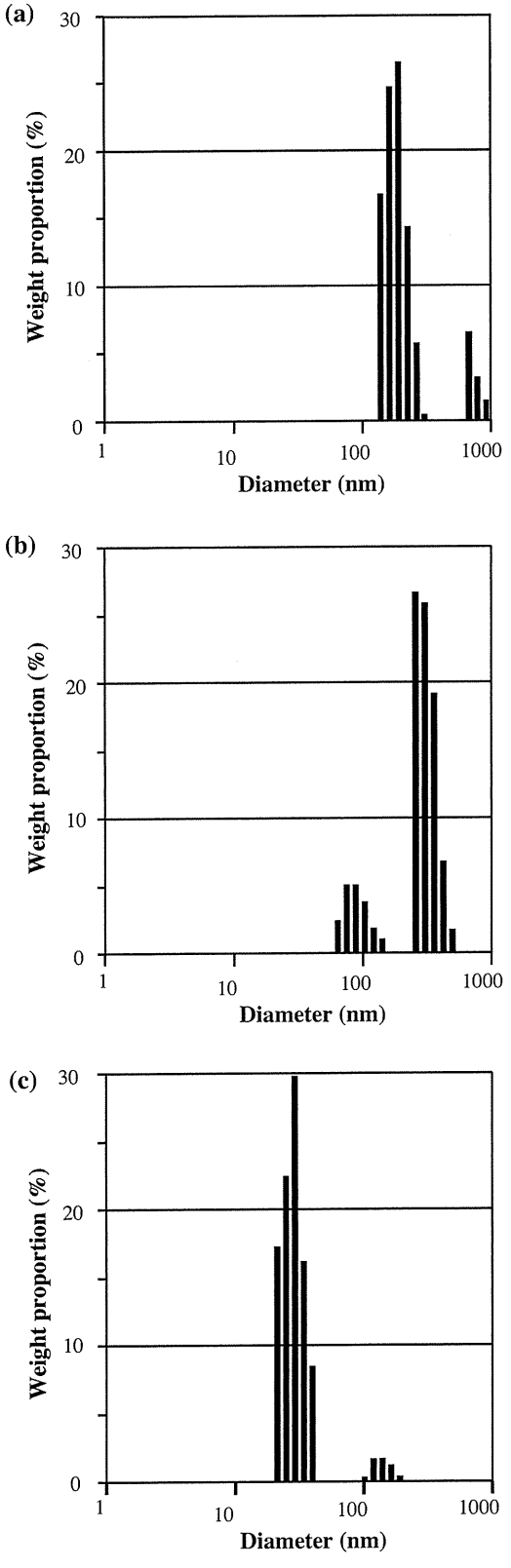

Fig. 3. Diameter distribution of PFC5-containing nano-emulsions (a and b) forming from PEG-P(Asp(C7F9)59) and empty polymeric micelle (c) measured by means of DLS. (a and b) are of different batches but prepared in the same conditions.

Using this polymer amount incorporated into the PFC-emulsions, we calculated the thickness of the polymer shell. We carried out the calculation with the following assumptions.

(1) The PFC-emulsions are made of the two phases; the inner PFC droplet phase and the outer polymer shell phase.
(2) We obtained PFC6 amounts in the emulsions assuming that sensitivity of PFC6 in gas chromatography is the same as that of PFC5. (The same peak area per PFC volume.)
(3) PFC6 and PFC5 are mixed freely without any gain or loss of droplet volume.
(4) Density of polymer is 1.03. (This is a common value of protein, and most synthetic polymers show similar values.)

The obtained value of the polymer shell's thickness was 22 nm, while the radius of the PFC droplet was 65 nm. In the future study, we like to analyse relationships between the shell thickness and physical stability of the emulsions.

3.2. Comparison with other emulsion-preparation methods

We compared the PFC5's concentrations of the PFC5-containing emulsions prepared in the sonication method with the PFC5's concentrations of the emulsions prepared in two common methods; mechanical stirring and high-pressure emulsification (Solans et al., 2005). We also compared the diameters of the emulsions prepared in the sonication method with those prepared in the two common methods. Previously, we reported PFC5-containing emulsions prepared by means of mechanical stirring that featured a magnetic stirrer (Nishihara et al., 2009). In this method, only the F-14% polymer provided a high PFC5 concentration (0.65 vol.%). The other polymers provided low or very low PFC5 concentrations: F-6% had 0.28 vol.%, F-22% had 0.19 vol.%, F-39% had 0.02 vol.%, and F-67% had 0.01 vol.%. In the F-14% case, the cumulant diameter was 694 nm, which was much larger than those obtained in the sonication method as described in the previous section (Section 3.1). Another distinct difference was found in a wide range of polymer compositions for high PFC5 concentrations in the sonication method. As summarized in runs 1–5 of Table 2, we compared the PFC5 concentrations (vol.%) and average diameters of the PFC5-containing emulsions for five polymer compositions. All these five compositions of polymers provided high PFC5 concentrations larger than 0.6 vol.%. Furthermore, all emulsion sizes of these runs (runs 2–5) were revealed to be small, at about 200 nm.

In the next step, we compared the sonication method with the most common method for emulsion preparation: high-pressure emulsification. For this comparison, we used F-15% polymer. We compared PFC5 concentrations and the cumulant average diameters of the emulsions prepared in the sonication method with PFC5 concentrations and the cumulant average diameters of the "high-pressure method" emulsions. We acquired a considerably high PFC5 concentration, 0.58 vol.%, by using a high-pressure emulsifier for the high-pressure emulsification method (its procedure is described in Section 2.3.1). However, the cumulant average diameter of the obtained emulsion was 477 nm. This value was much larger than the sonication-method value (232.4 nm, run 2 of Table 2). Additionally, maintenance of a low temperature at 4 °C for the whole instrument was essential in the high-pressure emulsification method, since possible heat generation due to the high-pressure process may considerably boost evaporation of PFC5 (the boiling temperature of PFC5 is 29 °C). In contrast, in the sonication method, a high PFC5 concentration was obtained at 40 °C, which is above PFC5's boiling temperature. (The temperature issue of the emulsion-preparation process will be more closely examined in the following section (Section 3.4).)

Please cite this article in press as: Shiraishi, K., et al., A facile preparation method of a PFC-containing nano-sized emulsion for theranostics of solid tumors. Int J Pharmaceut (2011), doi:10.1016/j.ijpharm.2011.10.006

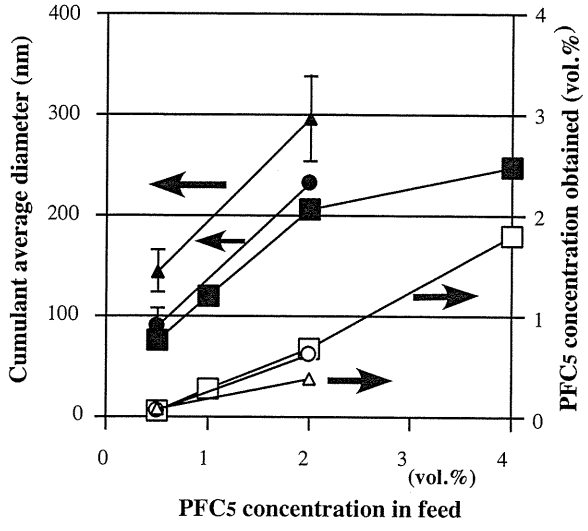

Fig. 4. Effects of polymer and PFC5 concentrations on physical properties of emulsions. PEG-P(Asp(C7F9)59) was used for emulsion preparations. Sample volume was 300 μL in 1.5-mL sample vials. Sonication was performed for 3 min at 40 °C. Filled plots represent cumulant average diameters, and vacant plots represent PFC5 concentrations of emulsions. Polymer concentration: △, ▲: 1.0 vol.%; ○, ●: 2.0 vol.%; □, ■: 4.0 vol.%.

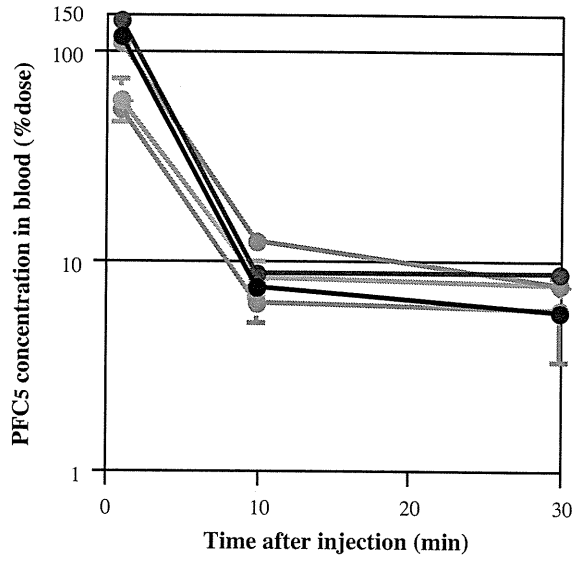

Fig. 5. Profiles of PFC5 concentration in blood. Black plot: run 1; blue plot: run 2; green plot: run 3; yellow plot: run 4; and red plot: run 5 (Table 5).

All these results indicate that the sonication method is a facile method for preparations of PFC5-containg emulsions with very small nano-sizes and high PFC5 concentrations.

3.3. Effects of sample volume, polymer concentration, and PFC5 concentration on incorporation behaviors

In the standard conditions, we put 300 μL water in a 1.5-mL of sealed glass tube and added polymer, PFC5, and PFC6. This configuration meant that a considerable amount of PFC5 perhaps would move from the solution into the glass tube's vacant atmospheric space (ca. 1.2 mL). We changed the volume of water while keeping constant the concentrations of polymer, PFC5, and PFC6 in the tube. Table 2 summarizes the results of runs 6–9 of Table 2. A higher PFC5 concentration was obtained in a case involving a larger water volume. (This means that there was a smaller vacant space in a sealed tube.) In accordance with the higher concentration of PFC5, the average diameter of the emulsion was observed to be larger. In run 9, PFC5's yield reached a very high value, approximately 90%. On the other hand, the PFC5's yield decreased to 32–33% when a small sample volume (300 μL) was adopted. These values indicate that the emulsification process can be well controlled through adjustment of sample volume.

Then, we examined effects that both polymer concentrations and PFC5 concentrations in feed had on the two physical values: diameter and PFC5 concentrations of the emulsion. Fig. 4 shows results of these two physical values for F-59% polymer cases. We changed the polymer concentration and the PFC5 concentration in feed in a range of 1.0–4.0 wt.% and of 0.5–4.0 vol.%, respectively. Each empty plot indicates PFC5 concentrations obtained for each polymer concentration, while each filled plot indicates cumulant average diameters for each polymer concentration. The polymer concentration was not found to significantly affect these two physical values. The polymer concentration affected very slightly the PFC5 content because three plot lines almost overlapped. When the polymer concentration was raised, only a small drop in the cumulant average diameter was observed. In contrast, the PFC5 concentration in feed was revealed to greatly affect the two physical values; larger values of PFC5 concentrations and cumulant average diameters were obtained with larger PFC5 concentrations in feed. Diameters of multi-modal distributions like Fig. 3(a) and (b) cannot be evaluated with the cumulant average diameters because the cumulant average diameters suppose the uni-modal diameter distribution. Therefore, we evaluated weight-weighted diameter distributions. Supplementary data, Table A summarizes and compares weight-weighted diameters with the cumulant average diameters. In most emulsion preparations, diameter distributions were found to be bi- or tri-modal, and therefore, exactly quantitative measurements of weight-weighted diameters are difficult in the homodyne analysis of dynamic light scattering done in this study. In fact, considerable differences are observed between the weight-weighted diameters and the cumulant average diameters for emulsions prepared in low PFC5 feed concentrations such as 1%, possibly due to the presence of empty polymeric micelles. (A DLS result of the empty micelle is shown in Fig. 3(c).) Even in this technical difficulty, the correlations obtained in Fig. 4a are not changed when multi-modal distributions are compared in the Supplementary data, Table A.

From the results obtained in this section, it was revealed that the sample volume and the PFC5 concentration in feed were appropriate factors for the facile control of size and the PFC5 content of the nano-sized emulsion.

3.4. Function of PFC6 in an emulsion preparation

In the above-described procedures for the emulsion preparation, we always used a 1:1 (vol./vol.) mixture of PFC5 and PFC6 in order to obtain a high PFC5 yield at a temperature higher than the boiling temperature of PFC5. We chose this 1:1 ratio because Kawabata et al. reported that ultrasound intensity required for the phase-transition (vaporization) induction at the 1:1 ratio was similar to that of a PFC5 alone case, and that this intensity was almost constant between ratios of 15:85, 50:50 (=1:1), and 85:15 (Asami et al., 2009). We varied temperatures (15, 25, 40, and 65 °C) of a sonicator's water bath, and performed the emulsion preparation both in the presence and the absence of PFC6 at each temperature. Table 3 summarizes results. In the absence of PFC6, PFC5 concentration was smaller than that of the corresponding PFC6-present case at every temperature. In runs 2 and 4, the obtained emulsions contained a considerable quantity of PFC5 over 0.2 vol.%. These two runs were prepared at lower temperatures than a boiling temperature of PFC5 (29 °C). Only a very small amount of PFC5

Please cite this article in press as: Shiraishi, K., et al., A facile preparation method of a PFC-containing nano-sized emulsion for theranostics of solid tumors. Int J Pharmaceut (2011), doi:10.1016/j.ijpharm.2011.10.006

Table 3
Effects of temperature and PFC6 addition on PFC5 incorporation behaviors.

Run	Temperature (°C)	PFC6 addition	PFC5 concentration (vol.%)[a]	Cumulant average diameter (nm)[a]
1	15	Yes	0.727 ± 0.191	210.8 ± 17.8
2	15	No	0.419 ± 0.124	82.7 ± 2.6
3	25	Yes	0.566 ± 0.367	177.1 ± 8.9
4	25	No	0.205 ± 0.086	95.7 ± 8.9
5[b]	40	Yes	0.634 ± 0.361	173.5 ± 24.5
6	40	No	0.049 ± 0.059	98.5 ± 5.1
7	65	Yes	0.154 ± 0.051	136.2 ± 16.0
8	65	No	0.096[c]	303.7[c]

[a] Average ± standard deviation ($n = 3$) except run 8.
[b] This run is identical to run 6 of Table 2.
[c] Average of two preparations.

was incorporated in run 6, which was performed at 40 °C, which is above PFC5's boiling temperature. This indicates that most PFC5 evaporated at 40 °C, and that interfacial Laplace pressure did not suppress PFC5's evaporation in the sonication procedure possibly because PFC5 evaporated from macroscopic PFC's droplets (in mm scale) before its incorporation into nano-emulsions where Laplace pressure's effect is great. In contrast, the PFC6-present cases presented similar amounts of PFC5 incorporated at 15, 25, and 40 °C. This means that PFC5's evaporation at 40 °C was efficiently suppressed through the mixing with PFC6. PFC5 and PFC6 not only are miscible but also these two compounds are expected to strongly interact with each other because these are both perfluorocarbons. It is considered that PFC5 evades evaporation through the strong interaction with PFC6 that has a higher boiling temperature than 40 °C. In run 7, performed at 65 °C, a considerable drop in the incorporated PFC5 amount was seen. This sonication temperature (65 °C) is higher than PFC6's boiling temperature (60 °C), and therefore, both PFC5 and PFC6 were evaporated at 65 °C. From these results, we have confirmed the function of the added PFC6 for high PFC5-incorporation amounts at a temperature higher than PFC5's boiling temperature.

3.5. PFC5 concentration profile in blood

We measured PFC concentrations in blood using several PFC5-containing emulsions in order to control their pharmacokinetic behaviors. For a larger amount of emulsion accumulation at tumor tissues, a longer half-life is preferable for a contrast agent. In contrast, a shorter half-life is advantageous for a diagnosis in a short period after injection of a contrast injection, since a low concentration of the contrast agent in blood is a pre-requisite for a high contrast image of the contrast agent's accumulated region. Under this contradictory situation for the optimum half-life, it is very important to obtain technologies to control (prolong and shorten) a half-life of the contrast agent.

We used three different types of polymers including PEG-P(Asp(C7F9)x) block copolymers in order to control half-livers in blood. In Table 4, we describe the compositions of the two copolymers other than PEG-P(Asp(C7F9)x). These two copolymers contain hydrophobic poly(L-lactic acid) chains that are expected to work for incorporation of hydrophobic PFC5 into emulsions. Table 5 summarizes five samples prepared from four polymers. By adjusting the vacant volume of a 1.5-mL glass vial to a small value (ca., 300 μL, meaning 1.2 mL of the sample volume.), we successfully obtained emulsions with higher PFC5 contents than 0.4 vol.% in runs 1–3. In these cases, the sonication was carried out at 15 °C. When emulsions were prepared in the same conditions of run 1 except for a different temperature (at 40 °C) and a different vacant volume (ca. 0 μL), the PFC5 content was considerably lower (0.408 vol.%) than in run 1.

Table 4
Compositions of two poly(L-lactic acid)(PLA)-containing polymers.

Code	Structure	Compositions
Gelatin derivative	Poly(L-lactic acid)-grafted gelatin	M.W. of PLA: 1000 weight ratio PLA/gelatin = 0.17
PEG-PLA	Poly(ethylene glycol)-b-Poly(L-lactic acid) Block copolymer	M.W. of PEG: 2000 M.W. of PLA: 1000

We injected these five samples in a mouse tail vein. As shown in Fig. 5, we observed a distinct difference in PFC5 concentrations at 1 min after the injection between three runs containing PLA (runs 1–3) and the other two runs for PEG-P(Asp(C7F9)x). The former three runs showed almost a 100% dose at 1 min with an assumption that blood volume was 7 vol./wt.% of body weight, while the latter two runs provided considerably smaller values than the 100% dose. In all runs, however, PFC5 concentrations were rapidly lowered at 10 and 30 min after the injection, and no clear difference was observed at these time points among all the runs. Therefore, control of pharmacokinetic behaviors, in particular prolongation of blood half-life from a few minutes, was not successfully achieved in this examination by the use of different polymer structures. For the pharmacokinetic control of the emulsions, an additional functional component may be required. Rapoport et al. (Rapoport et al., 2011) reported a very stable circulation (half-life = 2–4 h) in blood for perfluoro-crown-ether compound containing nano-emulsions.

Table 5
Compositions of PFC-emulsions for in vivo experiments.

Run	Polymer	Polymer concentration in feed (%)[a]	PFC5 concentration in feed (vol.%)	PFC5 concentration obtained in emulsion (vol.%)	Cumulant average diameter (nm)
1	Gelatin derivative[b]	1.0	1.25[d]	0.613	345.9
2	Gelatin derivative[b]	4.0	1.25[d]	0.429	542.6
3	PEG-b-PLA[a]	4.0	1.0[d]	0.491	222.6
4	F-15%[c]	4.0	2.0	0.465	256.3
5	F-59%[c]	4.0	1.0	0.670	225.1

[a] Weight (g)/water volume (mL).
[b] Listed in Table 4.
[c] Listed in Table 1.
[d] Sonication at 15 °C.

Please cite this article in press as: Shiraishi, K., et al., A facile preparation method of a PFC-containing nano-sized emulsion for theranostics of solid tumors. Int J Pharmaceut (2011), doi:10.1016/j.ijpharm.2011.10.006

According to this report, a perfluoro compound showing stable emulsion formation may be utilized for stable incorporation of another PFC.

4. Discussion

In the examinations of this study, we successfully obtained very small (ca. 200 nm in diameter) PFC5-containing emulsions with high PFC5 contents in a very facile method using a common bath-type sonicator. Actually, the used sonicator was the smallest model with the lowest sonication power (max. Input power: 90 W) in its product line. The other facile aspect of this preparation method is the working temperature. By mixing PFC6 we performed the emulsion preparation at 40 °C, which is above the boiling temperature of PFC5. In a conventional method's use of a high-pressure emulsifier, cooling of the whole system is required for evading a large amount evaporation of PFC5 due to heat generated within a high-pressure emulsifier. In contrast, we did not need cooling samples during the preparation. This facileness is substantially important when we consider a scale-up of the emulsion preparations. In a large-scale production of these emulsions, the heat generated in preparation processes (both in emulsification and sonication) may become large enough to raise a temperature of the solution above the boiling temperature. Therefore, successful preparations at a high temperature means that there is a large margin for large-scale preparation with high PFC5 content as well as easy handling of samples at room temperature throughout the sonication procedure.

We could not substantially change pharmacokinetic behaviors of the PFC5-containing emulsion, even when using different polymers. This is a very different situation from polymeric micelle drug carrier cases where block polymer structure was revealed to be a very influential factor on pharmacokinetic behaviors of the incorporated drug into the polymeric micelles (Yokoyama, 2005, 2007; Watanabe et al., 2006). This difference may result from the liquid state of the emulsion's core, while the solid core is essential for stable drug incorporation in the polymeric micelle systems. An alternative and novel method may be required to obtain stable incorporation of liquid PFC for dramatically changed pharmacokinetics.

5. Conclusion

By using a bath-type sonicator, we successfully obtained PFC5-containing emulsions in a diameter range of 200 nm. These emulsions are very potent for theranostics of solid tumors through ultrasound irradiation. Furthermore, these emulsions were prepared in high PFC5 yields at 40 °C, which is higher than the boiling temperature of PFC5. This very facile preparation method is an important technological key for large-scale production of these medically valuable emulsions.

Acknowledgements

This work was supported by the New Energy and Industrial Technology Development Organization, Japan. M. Yokoyama, K. Shiraishi, and M. Nishihara acknowledge support from the JST CREST program, Grant-in-Aid of the Ministry of Education, Culture, Sports, Science and Technology, Japan, and Kanagawa Academy of Science and Technology. The authors acknowledge Dr. Kenichi Kawabata and Dr. Rei Asami of Central Research Laboratory, Hitachi, Ltd., for their valuable discussion on PFC-containing nanoemulsions.

Appendix A. Supplementary data

Supplementary data associated with this article can be found, in the online version, at doi:10.1016/j.ijpharm.2011.10.006.

References

Ai, H., 2011. Layer-by-layer capsules for magnetic resonance imaging and drug delivery. Adv. Drug Deliv. Rev. 63, 772–788.
Asami, R., Azuma, T., Kawabata, K., 2009. Fluorocarbon droplets as next generation contrast agents—their behavior under 1–3 mhz ultrasound. IEEE Proc. Int. Ultrasonics Symp., 1294–1297.
Asami, R., Ikeda, T., Azuma, T., Kawabata, K., Umemura, S., 2010. Acoustic signal characterization of phase change nanodroplets in tissue-mimicking phantom gels. Jpn. J. Appl. Phys. 49, 07HF16.
Blanco, E., Kessinger, C.W., Sumer, B.D., Gao, J., 2009. Multifunctional micellar nanomedicine for cancer therapy. Exp. Biol. Med. 234, 123–131.
Bryson, J.M., Fichter, K.M., Chu, W.J., Lee, J.H., Li, J., Madsen, L.A., McLendon, P.M., Reineke, T.M., 2009. Polymer beacons for luminescence and magnetic resonance imaging of DNA delivery. Proc. Natl. Acad. Sci. U.S.A. 106, 16913–16918.
Chen, X.S., 2011. Introducing theranostics journal—from the editor-in-chief. Theranostics 1, 1–2.
Gianella, A., Jarzyna, P.A., Mani, V., Ramachandran, S., Calcagno, C., Tang, J., Kann, B., Dijk, W.J., Thijssen, V.L., Griffioen, A.W., Storm, G., Fayad, Z.A., Mulder, W.J., 2011. A multifunctional nanoemulsion platform for imaging guided therapy evaluated in experimental cancer. ACS Nano 5, 4422–4433.
Grishenkov, D., Pecorari, C., Brismar, T.B., Paradossi, G., 2009. Characterization of acoustic properties of PVA-shelled ultrasound contrast agents: ultrasound-induced fracture (part II). Ultrasound Med. Biol. 35, 1139–1147.
Hernot, S., Klibanov, A.L., 2008. Microbubbles in ultrasound-triggered drug and gene delivery. Adv. Drug Deliv. Rev. 60, 1153–1166.
Ishida, O., Maruyama, K., Sasaki, K., Iwatsuru, M., 1999. Size-dependent extravasation and interstitial localization of polyethyleneglycol liposomes in solid tumor-bearing mice. Int. J. Pharm. 190, 49–56.
Jeong, H., Huh, M., Lee, S.J., Koo, H., Kwon, I.C., Jeong, S.Y., Kim, K., 2011. Photosensitizer-conjugated human serum albumin nanoparticles for effective photodynamic therapy. Theranostics 1, 230–239.
Kaida, S., Cabral, H., Kumagai, M., Kishimura, A., Terada, Y., Sekino, M., Aoki, I., Nishiyama, N., Tani, T., Kataoka, K., 2010. Visible drug delivery by supramolecular nanocarriers directing to single-platformed diagnosis and therapy of pancreatic tumor model. Cancer Res. 70, 7031–7041.
Kalber, T.L., Kamaly, N., Higham, S.A., Pugh, J.A., Bunch, J., McLeod, C.W., Miller, A.D., Bell, J.D., 2011. Synthesis and characterization of a theranostic vascular disrupting agent for in vivo MR imaging. Bioconjug. Chem. 22, 879–886.
Kamaly, N., Miller, A.D., 2010. Paramagnetic liposome nanoparticles for cellular and tumour imaging. Int. J. Mol. Sci. 11, 1759–1776.
Kawabata, K., Sugita, N., Yoshikawa, H., Azuma, T., Umemura, S., 2005. Nanoparticles with multiple perfluorocarbons for controllable ultrasonically induced phase shifting. Jpn. J. Appl. Phys. 44, 4548–4552.
Kawabata, K., Asami, R., Yoshikawa, H., Azuma, T., Umemura, S., 2010a. Acoustic response of microbubbles derived from phase-change nanodroplet. Jpn. J. Appl. Phys. 49, 07HF18.
Kawabata, K., Asami, R., Yoshikawa, H., Azuma, T., Umemura, S., 2010b. Sustaining microbubbles derived from phase change nanodroplet by low-amplitude ultrasound exposure. Jpn. J. Appl. Phys. 49, 07HF20.
Kim, K., Kim, J.H., Park, H., Kim, Y.S., Park, K., Nam, H., Lee, S., Park, J.H., Park, R.W., Kim, I.S., Choi, K., Kim, S.Y., Park, K., Kwon, I.C., 2010. Tumor-homing multifunctional nanoparticles for cancer theragnosis: simultaneous diagnosis, drug delivery, and therapeutic monitoring. J. Contr. Rel. 146, 219–227.
Lammers, T., Kiessling, F., Hennink, W.E., Storm, G., 2010. Nanotheranostics and image-guided drug delivery: current concepts and future directions. Mol. Pharm. 7, 1899–1912.
Lammers, T., Aime, S., Hennink, W.E., Storm, G., Kiessling, F., 2011. Theranostic Nanomedicines. Acc. Chem. Res. 44, 1029–1038.
Litzinger, D.C., Buiting, A.M.J., van Rooijen, N., Huang, L., 1994. Effect of liposome size on the circulation time and intraorgan distribution of amphipathic poly(ethylene glycol)-containing liposomes. Biochim. Biophys. Acta 1190, 99–107.
MacKay, J.A., Li, Z., 2010. Theranostic agents that co-deliver therapeutic and imaging agents? Adv. Drug Deliv. Rev. 62, 1003–1004.
Min, K.H., Kim, J.H., Bae, S.M., Shin, H., Kim, M.S., Park, S., Lee, H., Park, R.W., Kim, I.S., Kim, K., Kwon, I.C., Jeong, S.Y., Lee, D.S., 2010. Tumoral acidic pH-responsive MPEG-poly(beta-amino ester) polymeric micelles for cancer targeting therapy. J. Contr. Rel. 144, 259–266.
Mohan, P., Rapoport, N., 2010. Doxorubicin as a molecular nanotheranostic agent: effect of doxorubicin encapsulation in micelles or nanoemulsions on the ultrasound-mediated intracellular delivery and nuclear trafficking. Mol. Pharm. 6, 1959–1973.
Moon, G.D., Choi, S.W., Cai, X., Li, W., Cho, E.C., Jeong, U., Wang, L.V., Xia, Y., 2011. A new theranostic system based on gold nanocages and phase-change materials with unique features for photoacoustic imaging and controlled release. J. Am. Chem. Soc. 133, 4762–4765.
Nagayasu, A., Uchiyama, K., Nishida, T., Yamagiwa, Y., Kawai, Y., Kiwada, H., 1996. Is control of distribution of liposomes between tumors and bone marrow possible? Biochim. Biophys. Acta 1278, 29–34.
Nakamura, E., Makino, K., Okano, T., Yamamoto, T., Yokoyama, M., 2006. A polymeric micelle MRI contrast agent with changeable relaxivity. J. Contr. Rel. 114, 325–333.
Nishihara, M., Imai, K., Yokoyama, M., 2009. Preparation of perfluorocarbon/fluoroalkyl polymer nanodroplets for cancer-targeted ultrasound contrast agents. Chem. Lett. 38, 556–557.

Please cite this article in press as: Shiraishi, K., et al., A facile preparation method of a PFC-containing nano-sized emulsion for theranostics of solid tumors. Int J Pharmaceut (2011), doi:10.1016/j.ijpharm.2011.10.006

Opanasopit, P., Yokoyama, M., Watanabe, M., Kawano, K., Maitani, Y., Okano, T., 2004. Block copolymer design for camptothecin incorporation into polymeric micelles for passive tumor targeting. Pharm. Res. 21, 2003–2010.
Pan, D., Caruthers, S.D., Hu, G., Senpan, A., Scott, M.J., Gaffney, P.J., Wickline, S.A., Lanza, G.M., 2008. Ligand-directed nanobialys as theranostic agent for drug delivery and manganese-based magnetic resonance imaging of vascular targets. J. Am. Chem. Soc. 130, 9186–9187.
Rapoport, N., Gao, Z., Kennedy, A., 2007. Multifunctional nanoparticles for combining ultrasonic tumor imaging and targeted chemotherapy. J. Natl. Cancer Inst. 99, 1095–1106.
Rapoport, N.Y., Kennedy, A.M., Shea, J.E., Scaife, C.L., Nam, K.H., 2009a. Controlled and targeted tumor chemotherapy by ultrasound-activated nanoemulsions/microbubbles. J. Contr. Rel. 138, 268–276.
Rapoport, N.Y., Nam, K.H., Gao, Z., Kennedy, A., 2009b. Application of ultrasound for targeted nanotherapy of malignant tumors. Acoust. Phys. 55, 594–601.
Rapoport, N., Christensen, D.A., Kennedy, A.M., Nam, K.H., 2010a. Cavitation properties of block copolymer stabilized phase-shift nanoemulsions used as drug carriers. Ultrasound Med. Biol. 36, 419–429.
Rapoport, N., Kennedy, A.M., Shea, J.E., Scaife, C.L., Nam, K.H., 2010b. Ultrasonic nanotherapy of pancreatic cancer: lessons from ultrasound imaging. Mol. Pharm. 7, 22–31.
Rapoport, N., Nam, K.H., Gupta, R., Gao, Z., Mohan, P., Payne, A., Todd, N., Liu, X., Kim, T., Shea, J., Scaife, C., Parker, D.L., Jeong, E.K., Kennedy, A.M., 2011. Ultrasound-mediated tumor imaging and nanotherapy using drug loaded, block copolymer stabilized perfluorocarbon nanoemulsions. J. Contr. Rel. 153, 4–15.
Sanson, C., Diou, O., Thévenot, J., Ibarboure, E., Soum, A., Brûlet, A., Miraux, S., Thiaudière, E., Tan, S., Brisson, A., Dupuis, V., Sandre, O., Lecommandoux, S., 2011. Doxorubicin loaded magnetic polymersomes: theranostic nanocarriers for MR imaging and magneto-chemotherapy. ACS Nano 5, 1122–1140.
Schutt, E.G., Klein, D.H., Mattrey, R.M., Riess, J.G., 2003. Injectable microbubbles as contrast agents for diagnostic ultrasound imaging: the key role of perfluorochemicals. Angew. Chem. Int. Ed. Engl. 42, 3218–3235.
Shiraishi, K., Kawano, K., Minowa, T., Maitani, Y., Yokoyama, M., 2009. Preparation and in vivo imaging of PEG-poly(L-lysine) -based polymeric micelle MRI contrast agents. J. Contr. Rel. 136, 14–20.
Shiraishi, K., Kawano, K., Maitani, Y., Yokoyama, M., 2010. Synthesis of Poly(ethylene glycol)-b-poly(L-lysine) block copolymers having Gd-DOTA as MRI contrast agent and their polymeric micelle formation by polyion complexation. J. Contr. Rel. 148, 160–167.
Solans, C., Izquierdo, P., Nolla, J., Azemar, N., Garcia-Celma, M.J., 2005. Nano-emulsions. Curr. Opin. Colloid Interface Sci. 10, 102–110.
Tadros, T., Izuquierdo, P., Esquena, J., Solans, C., 2004. Formation and stability of nano-emulsions. Adv. Colloid Interface. Sci. 108–109, 303–318.
Tanigo, T., Takaoka, R., Tabata, Y., 2010. Sustained release of water-insoluble simvastatin from biodegradable hydrogel augments bone regeneration. J. Contr. Rel. 143, 201–206.
Unger, E.C., Porter, T., Culp, W., Labell, R., Matsunaga, T., Zutshi, R., 2004. Therapeutic applications of lipid-coated microbubbles. Adv. Drug Deliv. Rev. 56, 1291–1314.
Yamamoto, T., Yokoyama, M., Opanasopit, P., Hayama, A., Kawano, K., Maitani, Y., 2007. What are determining factors for stable drug incorporation into polymeric micelle carriers? Consideration on physical and chemical characters of the micelle inner core. J. Contr. Rel. 123, 11–18.
Yokoyama, M., 2005. Polymeric micelles for the targeting of hydrophobic drugs. In: Kwon, G.S. (Ed.), Drug and Pharmaceutical Sciences, Polymeric Drug Delivery Systems, 148. Taylor & Francis, Boca Raton, pp. 533–575.
Yokoyama, M., 2007. Polymeric micelles as nano-sized drug carrier systems. In: Domb, A.J., Tabata, Y., Kumar, M.N.V.R., Farber, S. (Eds.), Nanoparticles for Pharmaceutical Applications. American Scientific Publishers, Stevenson Ranch, pp. 63–72.
Yokoyama, M., Opanasopit, P., Maitani, Y., Kawano, K., Okano, T., 2004. Polymer design and incorporation method for polymeric micelle carrier system containing water-insoluble anti-cancer agent camptothecin. J. Drug Target. 12, 373–384.
Yuan, F., Dellian, M., Fukumura, D., Leunig, M., Berk, D.A., Torchilin, V.P., Jain, R.K., 1995. Vascular permeability in a human tumor xenograft: molecular size dependence and cutoff size. Cancer Res. 55, 3752–3756.
Watanabe, M., Kawano, K., Yokoyama, M., Opanasopit, P., Okano, T., Maitani, Y., 2006. Preparation of camptothecin-loaded polymeric micelles and evaluation of their incorporation and circulation stability. Int. J. Pharm. 308, 183–189.

Please cite this article in press as: Shiraishi, K., et al., A facile preparation method of a PFC-containing nano-sized emulsion for theranostics of solid tumors. Int J Pharmaceut (2011), doi:10.1016/j.ijpharm.2011.10.006

molecular pharmaceutics

Article

pubs.acs.org/molecularpharmaceutics

Bubble Liposomes and Ultrasound Promoted Endosomal Escape of TAT-PEG Liposomes as Gene Delivery Carriers

Daiki Omata,[†] Yoichi Negishi,*[,†] Shoko Hagiwara,[†] Sho Yamamura,[†] Yoko Endo-Takahashi,[†] Ryo Suzuki,[‡] Kazuo Maruyama,[‡] Motoyoshi Nomizu,[§] and Yukihiko Aramaki[†]

[†]Department of Drug Delivery and Molecular Biopharmaceutics, School of Pharmacy, Tokyo University of Pharmacy and Life Sciences, Hachioji, Tokyo 192-0392, Japan

[‡]Department of Biopharmaceutics, School of Pharmaceutical Sciences, Teikyo University, Sagamihara, Kanagawa 252-5195, Japan

[§]Department of Clinical Biochemistry, School of Pharmacy, Tokyo University of Pharmacy and Life Sciences, Hachioji, Tokyo 192-0392, Japan

ABSTRACT: We have previously developed laminin-derived AG73 peptide-labeled poly(ethylene glycol)-modified liposomes (AG73-PEG liposomes) for selective cancer gene therapy and reported that Bubble liposomes (BLs) and ultrasound (US) exposure could accelerate the endosomal escape of AG73-PEG liposomes, leading to the enhancement of transfection efficiency; however, it is still unclear whether BLs and US exposure can also enhance the transfection efficiency of other vectors. We therefore assessed the effect of BLs and US exposure on the gene transfection efficiency of *trans*-activating transcriptor (TAT) peptide modified PEG liposomes. Although TAT-PEG liposomes were efficiently internalized into cells, the efficacy of endosomal escape was insufficient. The transfection efficiencies of TAT-PEG liposomes were enhanced by about 30-fold when BLs and US exposure were used. We also confirmed that BLs and US exposure could not enhance the direct transportation of TAT-PEG liposomes into cells. Confocal microscopy showed that BLs and US exposure promoted endosomal escape of TAT-PEG liposomes. Our results suggested that BLs and US exposure could enhance transfection efficiency by promoting endosomal escape, which was independent of modified molecules of carriers. Thus, BLs and US exposure can be a useful tool to achieve efficient gene transfection by improving endosomal escape of various carriers.

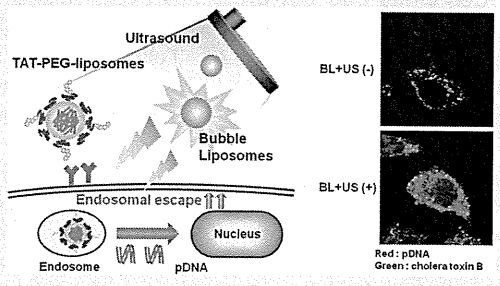

KEYWORDS: *Bubble liposomes, gene delivery, TAT peptide, ultrasound*

INTRODUCTION

Successful gene therapy depends on the efficient and safe delivery of genes into the desired tissues and cells. It is therefore necessary to develop efficient delivery vectors or methods for gene therapy. Nonviral vectors, such as cationic lipids or polymers, continue to be an attractive alternative to viral vectors due to their safety and convenient large-scale production, but their relatively low transfection efficiency compared with viral vectors is a major disadvantage.[1] In nonviral gene therapy, high transfection activity is required to improve the rate-limiting steps such as cellular internalization, endosomal escape, nuclear transfer, and intranuclear transcription.[2,3] In these steps, endosomal escape is considered one of the most important steps. When the vector cannot overcome this process, the cargo is degraded in lysosomes, leading to decreased gene transfection efficiency. For efficient endosomal escape, some studies have developed carriers equipped with functions such as pH sensitivity,[4,5] temperature dependence,[6] or photosensitivity.[7]

We have previously developed laminin-derived AG73 peptide-labeled poly(ethylene glycol) modified liposomes (AG73-PEG liposomes) for selective cancer gene therapy.[8] We also reported that echo-contrast gas-entrapping PEG liposomes, called "Bubble liposomes" (BLs), and ultrasound (US) exposure could accelerate the endosomal escape of AG73-PEG liposomes, leading to enhanced transfection efficiency.[9] It is expected that BLs and US exposure may promote the endosomal escape of various carriers and enhance their transfection efficiency; however, it is still unclear whether BLs and US exposure can enhance the transfection efficiency of vectors other than AG73-PEG liposomes, and the effect of BLs and US exposure on the transfection efficiency and endosomal escape of other functional molecule modified gene delivery carriers is not clearly understood.

Cell-penetrating peptides (CPPs), such as TAT and R8 peptides, are able to facilitate penetration through cell membranes and translocate different cargo into cells.[10] The TAT peptide, derived from a human immunodeficiency virus trans-acting transcriptional activator, has been studied to achieve highly efficient gene delivery and to develop TAT-modified liposomes and a polyplex.[11,12] The majority of these carriers were internalized via endocytosis and were required to achieve endosomal escape for efficient gene transfection.[13] Additionally, TAT-modified carriers equipped with components enhancing endosomal escape have been developed.[14]

Received: July 13, 2011
Revised: October 6, 2011
Accepted: October 24, 2011
Published: October 24, 2011

We therefore prepared TAT-modified liposomes as a model to evaluate the effect of BLs and US exposure on gene transfection efficiency via endosomal escape.

In this study, to assess the utility of BLs and US exposure for efficient gene delivery in general, we focused on TAT peptide and evaluated the effect of BLs and US exposure on the gene transfection efficiency of TAT-modified liposomes.

EXPERIMENTAL SECTION

Materials. The plasmid pCMV-Luc is an expression vector encoding the firefly luciferase gene under the control of cytomegalovirus promoter. Fluorescein isothiocyanate-conjugated cholera toxin B subunit (FITC-CTB), chloroquine, chlorpromazine and protamine were purchased from Sigma (St. Louis, MO). Cy3-labeled pDNA was purchased from Mirus Bio, LLC (Madison, WI). Genistein was purchased from Wako Pure Chemical Industries, Ltd. (Osaka, Japan). Amiloride was purchased from Calbiochem (San Diego, CA).

Cell Lines and Cultures. HeLa cells (human cervical cell line) were cultured in Dulbecco's modified Eagle's medium (DMEM; Kohjin Bio Co. Ltd., Tokyo, Japan), supplemented with 10% fetal bovine serum (FBS; Equitech Bio Inc., Kerrville, TX), penicillin (100 U/mL), and streptomycin (100 μg/mL) at 37 °C in a humidified 5% CO_2 atmosphere.

Preparation of TAT-PEG Liposomes. The Cys-TAT peptide (CGG-GRKKRRQRRRPPQ) was synthesized manually using the 9-fluorenylmethoxycarbonyl (Fmoc)-based solid-phase strategy, prepared in the COOH-terminal amide form and purified by reverse-phase high performance liquid chromatography. Liposomes were prepared by the hydration method. pDNA diluted in 10 mM HEPES buffer (pH 7.4) was condensed using protamine (N/P = 5.0). The complex of pDNA and protamine was added to a lipid film composed of 1,2-dioleoyl-*sn*-glycero-3-phospho-*rac*-1-glycerol (DOPG) (AVANTI Polar Lipids Inc., Alabaster, AL), 1,2-dioleoyl-*sn*-glycero-3-phosphoethanolamine (DOPE) (AVANTI Polar Lipids, Inc.), and 1,2-distearoyl-*sn*-glycero-3-phophatidylethanolamine-polyethyleneglycol-maleimide (DSPE-PEG_{2000}-Mal) (NOF Corporation, Tokyo, Japan) in a molar ratio of 2:9:0.57, followed by incubation for 10 min at room temperature to hydrate the lipids. The solution was sonicated for 5 min in a bath-type sonicator (42 kHz, 100 W) (2510J-DTH; Bransonic Ultrasonic Co., Danbury, CT). For coupling, TAT peptide, at a molar ratio of 5-fold DSPE-PEG_{2000}-Mal, was added to the PEG liposomes, and the mixture was incubated for 6 h at room temperature to conjugate the cysteine of the Cys-TAT peptide with the maleimide of the PEG liposomes using a thioether bond. The resulting TAT-peptide conjugated PEG liposomes (TAT-PEG liposomes) were dialyzed to remove any excess peptide. TAT-PEG liposomes were modified with 5 mol % PEG and 3 mol % peptides of total lipid. The particle size and ζ-potential of prepared liposomes were measured by NICOMP 380 ZLS (Particle Sizing Systems, Santa Barbara, CA).

Preparation of Bubble Liposomes. PEG liposomes composed of 1,2-dipalmitoyl-*sn*-glycero-3-phosphocholine (DPPC) (NOF Corporation) and 1,2-distearoyl-*sn*-glycero-3-phosphatidylethanolamine-poly(ethylene glycol) (DSPE-PEG_{2000}-OMe) (NOF Corporation) in a molar ratio of 94:6 were prepared by the reverse-phase evaporation method. In brief, all reagents were dissolved in 1:1 (v/v) chloroform/diisopropyl ether. Phosphate-buffered saline was added to the lipid solution, and the mixture was sonicated and then evaporated at 47 °C. The organic solvent was completely removed, and the size of the liposomes was adjusted to less than 200 nm using extruding equipment and a sizing filter (pore size: 200 nM) (Nuclepore Track-Etch Membrane; Whatman Plc, UK). The lipid concentration was measured using a phospholipid C test Wako (Wako Pure Chemical Industries, Ltd., Osaka, Japan). BLs were prepared from liposomes and perfluoropropane gas (Takachio Chemical Ind. Col. Ltd., Tokyo, Japan). First, 2 mL sterilized vials containing 0.8 mL of liposome suspension (lipid concentration: 1 mg/mL) were filled with perfluoropropane gas, capped, and then pressurized with a further 3 mL of perfluoropropane gas. The vial was placed in a bath-type sonicator (42 kHz, 100 W) (2510j-DTH; Branson Ultrasonics Co.) for 5 min to form BLs.

Transfection of pDNA into Cells Using TAT-PEG Liposomes. The day before the experiments, HeLa cells (3×10^4) were seeded in a 48-well plate. The cells were treated with TAT-PEG liposomes (encapsulated pDNA: 3 μg/mL) in serum-free medium for 4 h at 37 °C. After replacement with fresh medium, the cells were cultured for 20 h, and then luciferase activity was measured.

Transfection of pDNA into Cells by Combination of TAT-PEG Liposomes with BLs and US Exposure. The day before the experiments, HeLa cells (3×10^4) were seeded in a 48-well plate. The cells were treated with TAT-PEG liposomes (encapsulated pDNA: 3 μg/mL) in serum-free medium for 4 h at 37 °C. After incubation, the cells were washed twice within 10 min to remove any excess TAT-PEG liposomes that were not associated with the cells, and BLs (120 μg/mL) were added. Within 2 min, US exposure was applied through a 6 mm diameter probe placed in the well (frequency, 2 MHz; duty, 50%; burst rate, 2 Hz; intensity, 1.0 W/cm^2; time, 10 s). A Sonopore 3000 (NEPA GENE Co. Ltd., Chiba, Japan) was used to generate the US exposure. The cells were cultured for 20 h; then luciferase activity was determined, and cell viability was measured using a WST-8 assay (Cell Counting Kit-8; Dojindo Laboratories, Kumamoto, Japan).

Measurement of Luciferase Expression. Cell lysate was prepared with lysis buffer (0.1 M Tris-HCl (pH 7.8), 0.1% Triton X-100, and 2 mM EDTA). Luciferase activity was measured using a luciferase assay system (Promega) and a luminometer (LB96 V; Berthold Japan Co. Ltd., Tokyo, Japan). Activity is indicated as relative light units (RLU) per milligrams of protein.

Flow Cytometry Analysis. The day before the experiments, HeLa cells were seeded in a 12-well plate. Then, 0.2 mol % DiI-labeled TAT-PEG liposomes (pDNA: 3 μg/mL) were added to the cells and incubated for 1 h at 37 °C. The cells were collected, and the fluorescence intensities were measured by flow cytometry (FACSCanto; BD Biosciences, Franklin Lakes, NJ) to evaluate the cellular association of liposomes.

To examine the effect of BLs and US exposure on cellular uptake of pDNA, TAT-PEG liposomes (encapsulating Cy3-labeled pDNA: 3 μg/mL) were added to cells and incubated for 4 h at 37 °C. After incubation, the cells were washed twice, and BLs (120 μg/mL) were added. Then, US exposure was applied (frequency, 2 MHz; duty, 50%; burst rate, 2 Hz; intensity, 1.0 W/cm^2; time, 10 s). Subsequently, the cells were incubated for 10 or 60 min, and then the cells were collected by trypsinization and washed with PBS supplemented with heparin (50 μg/mL) three times to remove TAT-PEG liposomes and pDNA bound to the cell surface. The fluorescence intensity was measured by flow cytometry.

Confocal Laser Scanning Microscopy (CLSM). HeLa cells were seeded a day before the experiments. HeLa cells were

treated with TAT-PEG liposomes (Cy3-labeled pDNA: 3 μg/mL) and FITC-CTB (10 μg/mL) for 1 h at 37 °C. After incubation, the cells were washed, and BLs (120 μg/mL) were added. US exposure was then applied (frequency, 2028 kHz; duty, 50%; burst rate, 2.0 Hz; intensity, 1.0 W/cm^2; time, 10 s). Subsequently, the cells were incubated for 10, 60, or 180 min and then fixed with 4% paraformaldehyde for 1 h at 4 °C. CLSM was then performed (FV1000D; Olympus Corporation, Tokyo, Japan).

RESULTS

Characterization of Prepared TAT-PEG Liposomes. We evaluated the average size and zeta potential of prepared TAT-PEG liposomes, which were about 130 nm with a slight positive charge (Table 1).

Table 1. Characteristics of Prepared Liposomes[a]

prepared liposomes	PEG liposomes	TAT-PEG liposomes
particle size (nm)	132.1 ± 6.5	122.5 ± 10.5
ζ potential (mV)	3.17 ± 1.7	7.91 ± 1.6

[a]Data are the means and SD of three different determinations.

Cellular Association of TAT-PEG Liposomes. We first confirmed the effect of TAT peptide coating on the cellular association of liposomes and examined the association of TAT-PEG liposomes with HeLa cells. The cells were incubated with DiI-labeled liposomes for 1 h at 37 °C, and fluorescence intensity was determined by flow cytometry. The cellular internalization of TAT-PEG liposomes was observed by confocal laser scanning microscopy (CLSM). The cells treated with TAT-PEG liposomes showed increased fluorescence intensities compared with nonlabeled PEG liposomes (Figure 1A). In cells treated with TAT-PEG liposomes, the fluorescence of liposomes was observed in the cytoplasm, whereas it was weak in the cytoplasm of cells treated with nonlabeled PEG liposomes (Figure 1B). Furthermore, we investigated the cellular uptake pathway of TAT-PEG liposomes. Inhibitors that block clathrin-mediated endocytosis, raft-dependent endocytosis, and macropinocytosis were used to determine the cellular uptake pathway of TAT-PEG liposomes. Clathrin-mediated endocytosis was inhibited by chlorpromazine, which prevents the assembly of coated pits at the plasma membrane.[15] Raft-dependent endocytosis was inhibited by genistein, which is a thyrosine

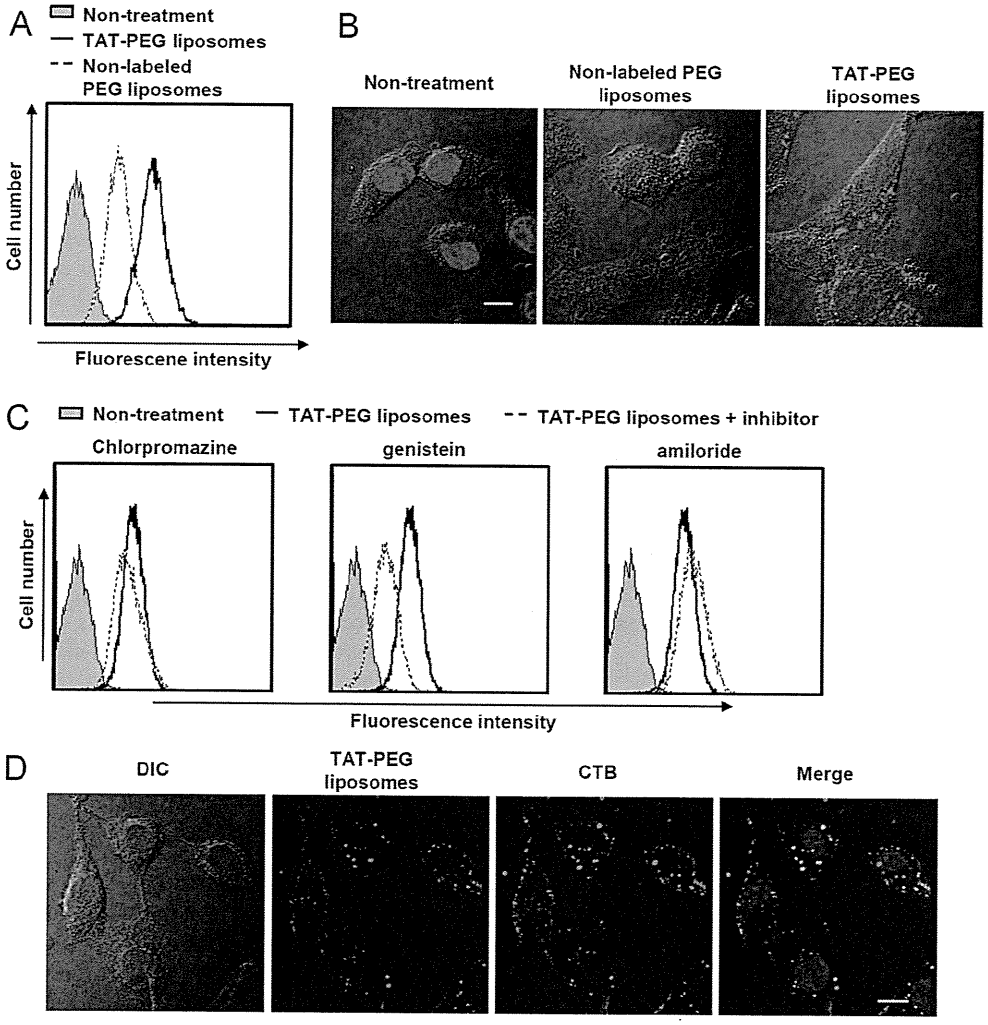

Figure 1. Cellular association of TAT-PEG liposomes. (A, B) HeLa cells were treated with DiI-labeled nonlabeled or TAT-PEG liposomes for 1 h at 37 °C. (A) The fluorescence intensity was measured by flow cytometry. (B) Cells were observed by CLSM. The scale bar represents 10 μm. (C) Cells were incubated with chlorpromazine (10 μg/mL), genistein (400 μM), or amiloride (1 mM) for 30 min and then treated with DiI-labeled TAT-PEG liposomes in the presence of an endocytic inhibitor for a further 1 h at 37 °C. Fluorescence intensities were measured by flow cytometry. (D) Cells were treated with DiI-labeled nonlabeled or TAT-PEG liposomes in the presence of FITC-CTB (10 μg/mL) for 1 h at 37 °C. Cells were observed by CLSM. The scale bar represents 10 μm.

dx.doi.org/10.1021/mp200353m | Mol. Pharmaceutics 2011, 8, 2416–2423

kinase inhibitor.[16] We also used amiloride, a specific inhibitor of the Na^+/H^+ exchange required for macropinocytosis.[17] Flow cytometry analysis showed that the fluorescence intensity of TAT-PEG liposomes in the cells was decreased when cells were treated with genistein. In contrast, the fluorescence intensity of TAT-PEG liposomes in the cells was not changed when cells were treated with chlorpromazine or amiloride (Figure 1C). Furthermore, to elucidate the intracellular localization of TAT-PEG liposomes, the cells were treated with DiI-labeled TAT-PEG liposomes and FITC-cholera toxin B subunit (FITC-CTB), a marker of raft-dependent endocytosis,[18] and then observed by CLSM. As a result, the fluorescence of TAT-PEG liposomes was colocalized with the fluorescence of CTB in cells treated with TAT-PEG liposomes and CTB for 1 h (Figure 1D).

Gene Transfection by TAT-PEG Liposomes. Although TAT-PEG liposomes could be internalized efficiently into cells via raft-dependent endocytosis, it was necessary to achieve high gene expression so that genes in the endosome were delivered into the cytoplasm. To assess the ability of endosomal escape in TAT-PEG liposomes, the cells were treated with TAT-PEG liposomes in the presence of chloroquine, which is recognized as an endosomolytic agent.[19] Luciferase activity was 100-fold higher than that following treatment with TAT-PEG liposomes in the absence of chloroquine (Figure 2). It was suggested that

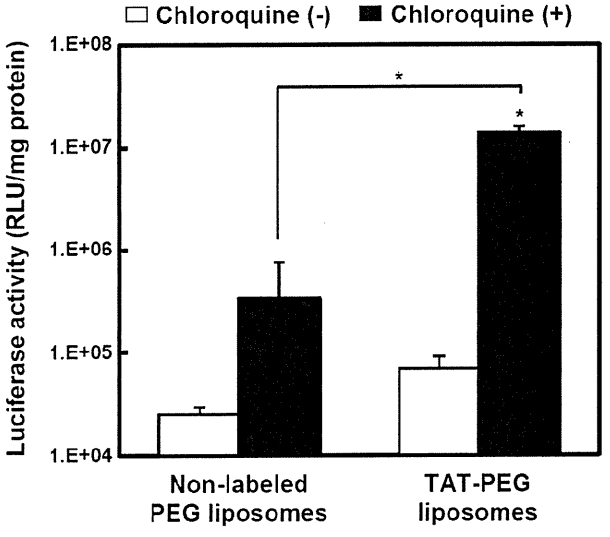

Figure 2. Gene transfection by TAT-PEG liposomes. Cells were preincubated with chloroquine (100 μM) for 30 min before transfection and then treated with nonlabeled or TAT-PEG liposomes in the presence of chloroquine for a further 4 h at 37 °C. After replacement with fresh medium, the cells were cultured for 20 h, and then luciferase activity was determined. Scale bars represent 10 μm. Data are the means ± SD (n = 4). *p < 0.05 compared with treatment in the absence of chloroquine.

the TAT-PEG liposomes prepared in this study could be efficiently internalized into cells but might not release genes into the cytoplasm from endosomes.

Effects of BLs and US Exposure on the Transfection Efficiency of TAT-PEG Liposomes. To investigate the effect of BLs and US exposure on TAT-mediated liposomal gene transfection, HeLa cells were treated with TAT-PEG liposomes for 4 h at 37 °C in a serum-free medium, and then the cells were treated with BLs and US exposure. After treatment with TAT-PEG liposomes, luciferase activity was enhanced up to 30-fold by BLs and US exposure compared with TAT-PEG liposomes alone. Furthermore, the combination of TAT-PEG liposomes with BLs and US exposure had about 10-fold higher luciferase activity than nonlabeled PEG liposomes with BLs and US exposure (Figure 3A). We also examined the transfection efficiency by treating TAT-PEG liposomes with US in the absence of BLs. As a result, the transfection efficiency was barely enhanced by treatment with TAT-PEG liposomes with US compared with TAT-PEG liposomes alone (Figure 3B). The cytotoxicity of the combination of TAT-PEG liposomes with or without BLs and US exposure was determined using a WST-8 assay. The cell viability was more than 80% even after each transfection (Figure 3C,D). It was suggested that BLs and US exposure could enhance the transfection efficiency of TAT-PEG liposomes without significant cytotoxicity.

Mechanism of Gene Transfection by TAT-PEG Liposomes with BLs and US Exposure. We examined the effects of BLs and US exposure on the cellular uptake of TAT-PEG liposomes. Flow cytometry analysis was performed to measure the fluorescence intensity of Cy3-labeled pDNA in cells transfected by TAT-PEG liposomes with or without BLs and US exposure. As a result, the cellular uptake of pDNA showed almost no difference in the presence of TAT-PEG liposomes with or without BLs and US exposure (Figure 4A). To evaluate the involvement of the direct induction of TAT-PEG liposomes into cells, the cells were transfected with TAT-PEG liposomes with or without BLs and US exposure at 37 or 4 °C. Twenty-three hours after transfection, luciferase activity was measured. When the cells were transfected by TAT-PEG liposomes with BLs and US exposure at 37 °C, the luciferase activity increased compared with that of cells treated with TAT-PEG liposomes alone. In contrast, luciferase activity did not change in cells treated with TAT-PEG liposomes with BLs and US exposure at 4 °C compared with TAT-PEG liposomes alone (Figure 4B). We also confirmed the effect of temperature on the cellular uptake of TAT-PEG liposomes. The cells were treated with DiI-labeled TAT-PEG liposomes for 1 h at 37 °C or at 4 °C, and then fluorescence intensity was measured by flow cytometry. In cells treated at 4 °C, fluorescence intensity decreased compared with cells treated at 37 °C (data not shown). To evaluate the intracellular distribution of pDNA, HeLa cells were treated with TAT-PEG liposomes containing Cy3-labeled pDNA in the presence of FITC-CTB for 1 h, and then the cells were treated with BLs and US exposure. After US exposure, the cells were incubated for 10, 60, or 180 min and observed by CLSM. In cells treated with TAT-PEG liposomes alone, the fluorescence of pDNA colocalized with the fluorescence of CTB. In contrast, when cells were treated with BLs and US exposure, the fluorescence of CTB was dispersed widely in cells that were incubated for 10 min after US exposure (Figure 4C). We also confirmed the intracellular distribution of pDNA and CTB in living cells. As a result, the distribution of pDNA and CTB in living cells was similar to that of fixed cells (data not shown). Furthermore, we examined the intracellular distribution of pDNA and CTB treated by TAT-PEG liposomes with US in the absence of BLs. The intracellular distribution of pDNA and CTB showed almost no difference between the treatment of TAT-PEG liposomes alone and TAT-PEG liposomes with US exposure without BLs (data not shown).

It was suggested that BLs and US exposure could affect the intracellular trafficking of pDNA and enhance the transfection efficacy of TAT-PEG liposomes.

dx.doi.org/10.1021/mp200353m | Mol. Pharmaceutics 2011, 8, 2416–2423

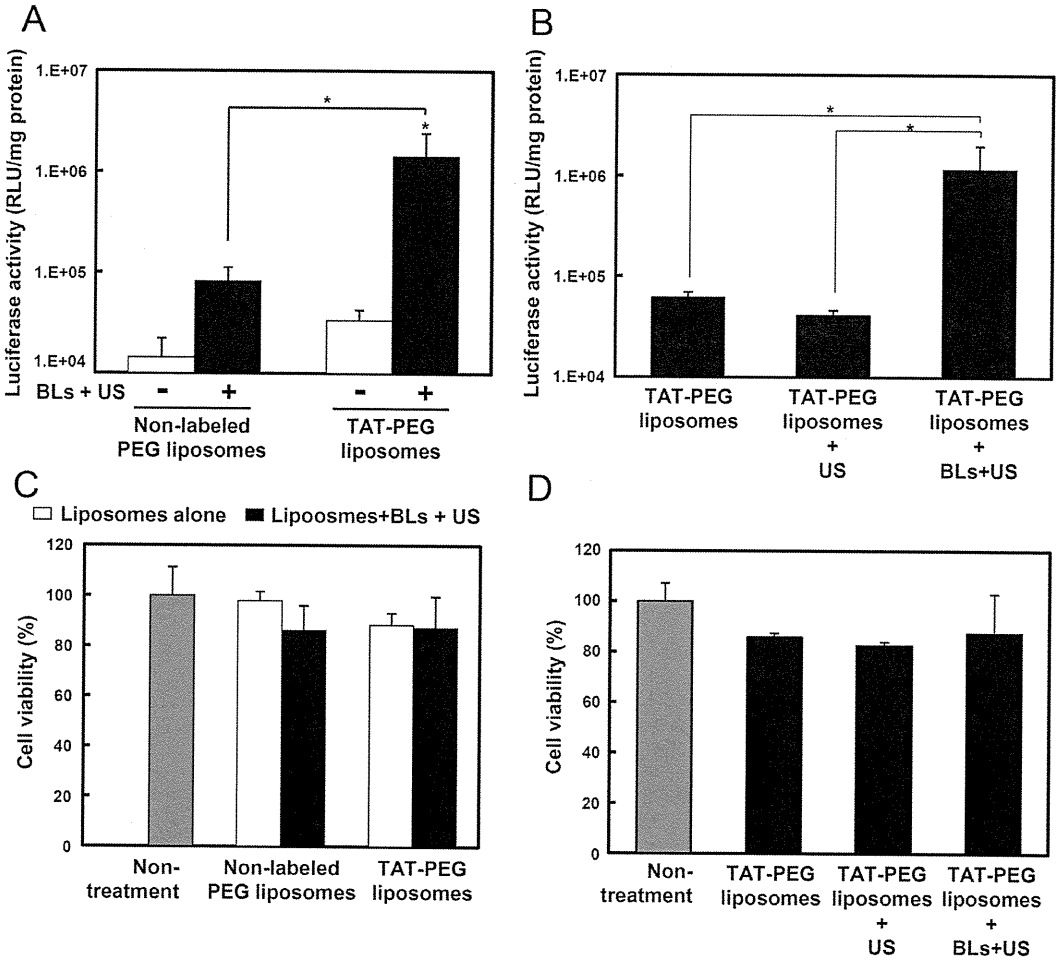

Figure 3. Effect of BLs and US exposure on TAT-mediated liposomal gene transfection. HeLa cells were treated with nonlabeled or TAT-PEG liposomes for 4 h. The cells were then washed and treated with or without BLs (120 μg/mL) and US exposure. They were incubated for 20 h; then (A, B) luciferase activity was determined, and (C, D) cell viability was measured using a WST-8 assay. Data are the means ± SD (n = 4). *p < 0.05 compared with TAT-PEG liposomes alone.

DISCUSSION

Recent studies have suggested that endosomal escape is important to achieve efficient gene delivery.[2,3] We have previously reported that BLs and US exposure could improve the transfection efficiency of laminin-derived AG73-PEG liposomes containing pDNA by promoting endosomal escape.[9] In this report, we demonstrated that BLs and US exposure could enhance not only the transfection efficiency of AG73-PEG liposomes but also that of TAT-PEG liposomes.

For efficient gene delivery, various moieties were used to develop carriers which enhance cellular internalization or selectivity. CPPs, such as TAT, R8, or penetratin, were used to achieve efficient gene internalization.[12,20,21] On the other hand, for selective gene delivery, folate, transferrin, RGD, or anisamide was used as a ligand.[22−25] These moieties were associated with a specific receptor and internalized via several endocytoses. TAT peptide was associated with heparan sulfate proteoglycan, which has been controversial.[26] In addition, some studies have developed TAT peptide-modified carriers, which were equipped with components enhancing endosomal escape;[14] therefore, we focused on TAT peptide and evaluated whether BLs and US exposure can enhance the transfection efficiency of TAT peptide-modified carriers to demonstrate the utility of BLs and US exposure in general. The present results showed that BLs and US exposure could enhance the gene transfection efficiency of TAT-PEG liposomes (Figure 3A). Furthermore, although we have previously reported that AG73-PEG liposomes were partially internalized via clathrin-mediated endocytosis,[9] the TAT-PEG liposomes prepared in this study were mostly internalized via a raft-dependent endocytic pathway (Figure 1C). These results suggested that BLs and US exposure could enhance the transfection efficiency of vectors, which were internalized via various receptor and endocytic pathways; however, further studies are needed to evaluate the effect of BLs and US exposure on the transfection efficiency of vectors, which were internalized via various endocytic pathways, such as macropinocytosis.

For successful gene therapy, nonviral vectors could be needed to overcome rate-limiting steps, such as cellular internalization, endosomal escape, and nuclear transfer.[2,3] Endosomal escape is considered to be one of the most important steps. Although PEG modification was considered a useful component to increase the stability of vectors in vivo, it also inhibited endosomal escape, leading to decreased gene expression.[27,28] Our results also showed that TAT-PEG liposomes could not escape from endosomes to the cytosol efficiently (Figures 1D, 2). We previously reported that BLs and US exposure could enhance the endosomal escape of AG73-PEG liposomes.[9] We therefore further confirmed the effect of BLs and US exposure on endosomal escape of TAT-PEG liposomes. We and other

dx.doi.org/10.1021/mp200353m | Mol. Pharmaceutics 2011, 8, 2416–2423

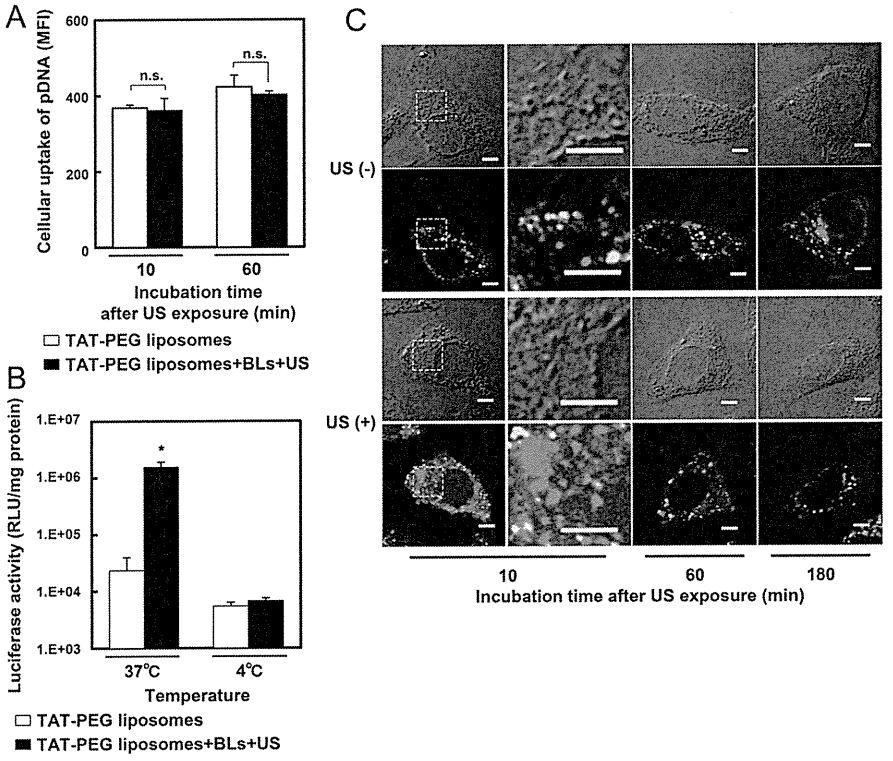

Figure 4. Mechanism of accelerated TAT-mediated liposomal gene transfection by BLs and US exposure. (A) HeLa cells were incubated with TAT-PEG liposomes encapsulating Cy3-labeled pDNA for 4 h at 37 °C. After incubation, the cells were washed, and BLs were added. Then the cells were exposed to US and incubated for 10 or 60 min. The cells were then collected and washed with heparin-containing PBS three times. The fluorescence intensity was measured by flow cytometry. Data are shown as the means ± SD (n = 3). (B) Cells were preincubated for 30 min at either 37 or 4 °C before transfection and then treated with TAT-PEG liposomes for a further 1 h at 37 or 4 °C. After incubation, the cells were washed, and BLs were added. The cells were then exposed to US and cultured for 23 h. Luciferase activity was determined. Data are the means ± SD (n = 4). *p < 0.05 compared with TAT-PEG liposomes alone. (C) Cells were treated with TAT-PEG liposomes encapsulating Cy3-labeled pDNA and FITC-CTB (10 μg/mL) for 1 h at 37 °C. After incubation, the cells were washed, and BLs were added. The cells were then exposed to US, incubated for 10, 60, 180 min, and then fixed with 4% paraformaldehyde for 1 h at 4 °C and observed by CLSM. The areas surrounded by dotted line are shown as enlarged images. Scale bars represent 5 μm.

groups have reported that the combination of BLs or microbubbles with US exposure could increase cell membrane permeability and deliver genes into the cytosol directly;[29−33] however, our results indicated that enhanced transfection efficiency did not rely on the increase of the direct cellular uptake of TAT-PEG liposomes, which is associated with the cell membrane (Figure 4A). In addition, CLSM analysis showed that BLs and US exposure could affect intracellular trafficking of TAT-PEG liposomes. Although endocytic vesicles labeled with FITC-CTB were observed as punctuate structures, when BLs and US exposure was applied, it was observed that FITC-CTB diffused into the cytosol (Figure 4B). These results suggested that BLs and US exposure could accelerate endosomal escape of TAT-PEG liposomes. We also examined whether sonazoid (Daiichi-Sankyo Pharmaceuticals, Tokyo, Japan) and US exposure could enhance the transfection efficiency of TAT-PEG liposomes. Sonazoid consists of perfluorobutane gas microbubbles stabilized by a monolayer membrane of hydrogenated egg phosphatidyl serine.[34] As a result, the transfection efficiency of TAT-PEG liposomes was enhanced by sonazaoid and US exposure (data not shown). This result suggested that microbubbles and US exposure could enhance the gene transfection efficiency of gene delivery carriers.

We also prepared folate-PEG liposomes containing pDNA and examined whether BLs and US exposure could enhance the transfection efficiency of folate-PEG liposomes. Folate, a high-affinity ligand for folate receptor, has been widely used as a ligand for selective gene delivery, and folate-modified carriers required various components enhancing endosomal escape to achieve high gene transfection efficiency.[35] We confirmed that folate-PEG liposomes had relatively low transfection efficiency because of the lower ability of endosomal escape, but when BLs and US exposure was used with folate-PEG liposomes, the transfection efficiency of folate-PEG lisposomes was enhanced (data not shown). These findings also suggested that BLs and US exposure could enhance the endosomal escape of gene delivery vectors, leading to increased gene expression.

We have reported that the transfection efficiency of AG73-PEG liposomes using BLs and US exposure was enhanced 60-fold,[9] whereas that of TAT-PEG liposomes was up-regulated 12-fold (Figure 3A). These results suggested that BLs and US exposure could easily influence the intracellular trafficking of AG73-PEG liposomes compared to TAT-PEG liposomes. The different efficacy of endosomal escape between AG73-PEG liposomes and TAT-PEG liposomes might be dependent on the difference of the receptor, endocytic pathway of carrier, and the type of cells. The responsibility of BLs and US exposure to individual cells might also affect the efficiency of endosomal escape, leading to different transfection efficiencies; therefore, it is important to clarify the mechanism of the different efficacy of endosomal escape of these carriers. However, we expect that this method of promoting endosomal escape using BLs and US

dx.doi.org/10.1021/mp200353m | Mol. Pharmaceutics 2011, 8, 2416–2423

exposure may also be applied to existing carriers for drug, peptide, or protein delivery, which have low intracellular delivery efficacy due to poor endosomal escape.

In further studies, we will attempt to demonstrate the detailed mechanism of enhanced endosomal escape of carriers by treatment with BLs and US exposure. It has been demonstrated that microbubbles and US exposure induce several biological effects, such as influx of calcium ions or generation of reactive oxygen species.[36−39] It has been also reported that endosomal acidification is adjusted by calcium ions;[40] therefore, we will assess whether the influx of calcium ions induced by BLs and US exposure affects endosomal acidification and function, leading to the destabilization of endosomes and enhancement of endosomal escape. On the other hand, we may also need to elucidate more clearly the effect of BLs and US exposure on transcription and other organelles. Although it is possible that BLs and US exposure may induce several biological effects involved in gene expression, BLs and US exposure could affect the intracellular distribution of pDNA and CTB (Figure 4); therefore, our results suggested that BLs and US exposure could certainly improve at least the endosomal escape of TAT-PEG liposomes.

In conclusion, as schematically shown in Figure 5, TAT-PEG liposomes were internalized into cells via HSPG and raft-dependent endocytosis. On the other hand, AG73-PEG liposomes and folate-PEG liposomes were internalized via syndecan-2 and folate receptor, respectively. When BLs and US exposure were applied, endosomal escape was enhanced, leading to increased transfection efficiency of these carriers. These results suggested that BLs and US exposure could enhance transfection efficiency by promoting endosomal escape, which was independent of the receptors and endocytic pathway of carriers. Thus, BLs and US exposure can be useful tools to achieve efficient gene transfection by improving endosomal escape using various carriers.

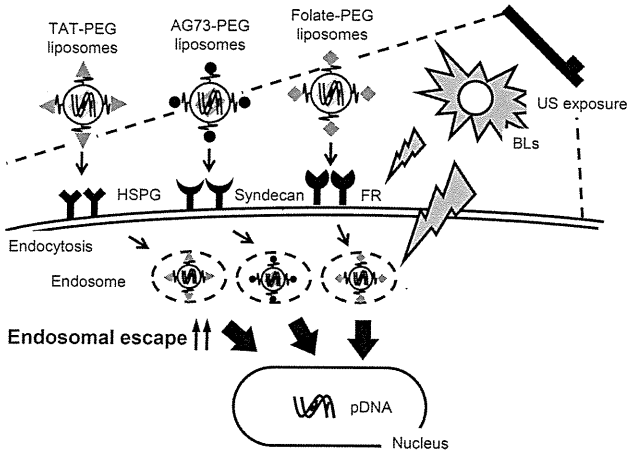

Figure 5. Diagram of enhanced gene delivery by BLs and US exposure. Several moiety-modified gene delivery carriers were internalized into cells via receptors and the endocytic pathway. When BLs and US exposure were applied, endosomal escape was enhanced, leading to increased transfection efficiency, which was independent of the receptor and endocytic pathway of carriers. HSPG, heparan sulfate proteoglycan; FR, folate receptor; US, ultrasound; BLs, Bubble liposomes; PEG, poly(ethylene glycol).

AUTHOR INFORMATION

Corresponding Author

*Mailing address: Tokyo University of Pharmacy and Life Sciences, School of Pharmacy, 1432-1 Horinouchi, Hachioji, Tokyo 192-0392, Japan. Tel. and fax: +81-42-676-3183. E-mail address: negishi@toyaku.ac.jp (Y.N.).

ACKNOWLEDGMENTS

We are grateful to Dr. Katsuro Tachibana (Department of Anatomy, School of Medicine, Fukuoka University) for technical advice regarding the induction of cavitation with US and to Mr. Yasuhiko Hayakawa, Mr. Takahiro Yamauchi, and Mr. Kosho Suzuki (NEPA GENE CO., LTD.) for technical advice regarding exposure to US. This study was supported by an Industrial Technology Research Grant (04A05010) from the New Energy and Industrial Technology Development Organization (NEDO) of Japan, Grant-in-Aid for Exploratory Research (18650146) and Grant-in-Aid for Scientific Research (B) (20300179) from the Japan Society for the Promotion of Science, and by a grant for private universities provided by the Promotion and Mutual Aid Corporation for Private Schools of Japan.

ABBREVIATIONS

BLs, Bubble liposomes; CTB, cholera toxin B subunit; DOPE, 1,2-dioleoyl-sn-glycero-3-phosphoethanolamine; DOPG, 1,2-dioleoyl-*sn*-glycero-3-phospho-*rac*-1-glycerol; DSPE, 1,2-distearoyl-*sn*-glycero-3-phosphatidyl-ethanolamine; FBS, fetal bovine serum; Fmoc, fluorenylmethoxycarbonyl; Mal, maleimide; pDNA, plasmid DNA; PEG, poly(ethylene glycol); US, ultrasound

REFERENCES

(1) Zhang, S.; Xu, Y.; Wang, B.; Qiao, W.; Liu, D.; Li, Z. Cationic compounds used in lipoplexes and polyplexes for gene delivery. *J. Controlled Release* **2004**, *100*, 165−180.

(2) Hama, S.; Akita, H.; Ito, R.; Mizuguchi, H.; Hayakawa, T.; Harashima, H. Quantitative comparison of intracellular trafficking and nuclear transcription between adenoviral and lipoplex systems. *Mol. Ther.* **2006**, *13*, 786−794.

(3) Varga, C. M.; Tedford, N. C.; Thomas, M.; Klibanov, A. M.; Griffith, L. G.; Auffenburger, D. A. Quantitative comparison of polyethylenimine formulations and adenoviral vectors in terms of intracellular gene delivery processes. *Gene Ther.* **2005**, *12*, 1023−1032.

(4) Hatakeyama, H.; Ito, E.; Akita, H.; Oishi, M.; Nagasaki, Y.; Futaki, S.; Harashima, H. A pH-sensitive fusogenic peptide facilitates endosomal escape and greatly enhances the gene silencing of siRNA-containing nanoparticles in vitro and in vivo. *J. Controlled Release* **2009**, *139*, 127−132.

(5) Subbarao, N. K.; Parente, R. A.; Szoka, F. C.; Nadasdi, L.; Pongracz, K. pH-dependent bilayer destabilization by an amphipathic peptide. *Biochemistry* **1987**, *26*, 2964−2972.

(6) Lee, S. H.; Choi, S. H.; Kim, S. H.; Park, T. G. Thermally sensitive cationic polymer nanocapsules for specific cytosolic delivery and efficient gene silencing of siRNA: swelling induced physical disruption of endosome by cold shock. *J. Controlled Release* **2008**, *125*, 25−32.

(7) Høgset, A.; Prasmickaite, L.; Selbo, P. K.; Hellum, M.; Engesaeter, B. Ø.; Bonsted, A.; Berg, K. Photochemical internalisation in drug and gene delivery. *Adv. Drug Delivery Rev.* **2004**, *56*, 95−115.

(8) Negishi, Y.; Omata, D.; Iijima, H.; Hamano, N.; Endo-Takahashi, Y.; Nomizu, M.; Aramaki, Y. Preparation and characterization of laminin-derived peptide AG73-coated liposomes as a selective gene delivery tool. *Biol. Pharm. Bull.* **2010**, *33*, 1766−1769.

(9) Negishi, Y.; Omata, D.; Iijima, H.; Takabayashi, Y.; Suzuki, K.; Endo, Y.; Suzuki, R.; Maruyama, K.; Nomizu, M.; Aramaki, Y. Enhanced laminin-derived peptide AG73-mediated liposomal gene transfer by Bubble liposomes and ultrasound. *Mol. Pharmaceutics* **2010**, *7*, 217–226.

(10) Katayama, S.; Hirose, H.; Takayama, K.; Nakase, I.; Futaki, S. Acylation of octaarginine: Implication to the use of intracellular delivery vectors. *J. Controlled Release* **2011**, *149*, 29–35.

(11) Dey, D.; Inayathullah, M.; Lee, A. S.; Lemieux, M. C.; Zhang, X.; Wu, Y.; Nag, D.; De Almeida, P. E.; Han, L.; Rajadas, J.; Wu, J. C. Efficient gene delivery of primary human cells using peptide linked polyethylenimine polymer hybrid. *Biomaterials* **2011**, *32*, 4647–4658.

(12) Yamano, S.; Dai, J.; Yuvienco, C.; Khapli, S.; Moursi, A. M.; Montclare, J. K. Modified Tat peptide with cationic lipids enhances gene transfection efficiency via temperature-dependent and caveolae-mediated endocytosis. *J. Controlled Release* **2011**, *152*, 278–285.

(13) Zeng, X.; Sun, Y. X.; Qu, W.; Zhang, X. Z.; Zhuo, R. X. Biotinylated transferrin/avidin/biotinylated disulfide containing PEI bioconjugates mediated p53 gene delivery system for tumor targeted transfection. *Biomaterials* **2010**, *31*, 4771–4780.

(14) Suk, J. S.; Suh, J.; Choy, K.; Lai, S. K.; Fu, J.; Hanes, J. Gene delivery to differentiated neurotypic cells with RGD and HIV Tat peptide functionalized polymeric nanoparticles. *Biomaterials* **2006**, *27*, 5143–5150.

(15) Wang, L. H.; Rothberg, K. G.; Anderson, R. G. Mis-assembly of clathrin lattices on endosomes reveals a regulatory switch for coated pit formation. *J. Cell. Biol.* **1993**, *123*, 1107–1117.

(16) Pelkmans, L.; Püntener, D.; Helenius, A. Local actin polymerization and dynamin recruitment in SV40-induced internalization of caveolae. *Science* **2002**, *296*, 535–539.

(17) Wadia, J. S.; Stan, R. V.; Dowdy, S. F. Transducible TAT-HA fusogenic peptide enhances escape of TAT-fusion proteins after lipid raft macropinocytosis. *Nat. Med.* **2004**, *10*, 310–315.

(18) Janes, P. W.; Ley, S. C.; Magee, A. I. Aggregation of lipid rafts accompanies signaling via the T cell antigen receptor. *J. Cell. Biol.* **1999**, *147*, 447–461.

(19) Sonawane, N. D.; Szoka, F. C.; Verkman, A. S. Chloride accumulation and swelling in endosomes enhances DNA transfer by polyamine-DNA polyplexes. *J. Biol. Chem.* **2003**, *278*, 44826–44831.

(20) Kibria, G.; Hatakeyama, H.; Ohga, N.; Hida, K.; Harashima, H. Dual-ligand modification of PEGylated liposomes shows better cell selectivity and efficient gene delivery. *J. Controlled Release* **2011**, *153*, 141–148.

(21) Mäe, M.; El Andaloussi, S.; Lundin, P.; Oskolkov, N.; Johansson, H. J.; Guterstam, P.; Langel, U. A stearylated CPP for delivery of splice correcting oligonucleotides using a non-covalent co-incubation strategy. *J. Controlled Release* **2009**, *134*, 221–227.

(22) Morris, V. B.; Sharma, C. P. Folate mediated l-arginine modified oligo (alkylaminosiloxane) graft poly(ethyleneimine) for tumor targeted gene delivery. *Biomaterials* **2011**, *32*, 3030–3041.

(23) Koppu, S.; Oh, Y. J.; Edrada-Ebel, R.; Blatchford, D. R.; Tetley, L.; Tate, R. J.; Dufes, C. Tumor regression after systemic administration of a novel tumor-targeted gene delivery system carrying a therapeutic plasmid DNA. *J. Controlled Release* **2010**, *143*, 215–221.

(24) Ng, Q. K.; Sutton, M. K.; Soonsawad, P.; Xing, L.; Cheng, H.; Segura, T. Engineering clustered ligand binding into nonviral vectors: $\alpha v\beta 3$ targeting as an example. *Mol. Ther.* **2009**, *17*, 828–836.

(25) Li, S. D.; Chono, S.; Huang, L. Efficient oncogene silencing and metastasis inhibition via systemic delivery of siRNA. *Mol. Ther.* **2008**, *16*, 942–946.

(26) Imamura, J.; Suzuki, Y.; Gonda, K.; Roy, C. N.; Gatanaga, H.; Ohuchi, N.; Higuchi, H. Single Particle Tracking Confirms That Multivalent Tat Protein Transduction Domain-induced Heparan Sulfate Proteoglycan Cross-linkage Activates Rac1 for Internalization. *J. Biol. Chem.* **2011**, *286*, 10581–10592.

(27) Hatakeyama, H.; Akita, H.; Kogure, K.; Oishi, M.; Nagasaki, Y.; Kihira, Y.; Ueno, M.; Kobayashi, H.; Kikuchi, H.; Harashima, H. Development of a novel systemic gene delivery system for cancer therapy with a tumor-specific cleavable PEG-lipid. *Gene Ther.* **2007**, *14*, 68–77.

(28) Walker, G. F.; Fella, C.; Pelisek, J.; Fahrmeir, J.; Boeckle, S.; Ogris, M.; Wagner, E. Toward synthetic viruses: endosomal pH-triggered deshielding of targeted polyplexes greatly enhances gene transfer in vitro and in vivo. *Mol. Ther.* **2005**, *11*, 418–425.

(29) Negishi, Y.; Matsuo, K.; Endo-Takahashi, Y.; Suzuki, K.; Matsuki, Y.; Takagi, N.; Suzuki, R.; Maruyama, K.; Aramaki, Y. Delivery of an angiogenic gene into ischemic muscle by novel Bubble liposomes followed by ultrasound exposure. *Pharm. Res.* **2011**, *28*, 712–719.

(30) Suzuki, R.; Namai, E.; Oda, Y.; Nishiie, N.; Otake, S.; Koshima, R.; Hirata, K.; Taira, Y.; Utoguchi, N.; Negishi, Y.; Nakagawa, S.; Maruyama, K. Cancer gene therapy by IL-12 gene delivery using liposomal bubbles and tumoral ultrasound exposure. *J. Controlled Release* **2010**, *142*, 245–250.

(31) Lentacker, I.; Wang, N.; Vandenbroucke, R. E.; Demeester, J.; De Smedt, S. C.; Sanders, N. N. Ultrasound Exposure of Lipoplex Loaded Microbubbles Facilitates Direct Cytoplasmic Entry of the Lipoplexes. *Mol. Pharmaceutics* **2009**, *6*, 457–467.

(32) Negishi, Y.; Endo, Y.; Fukuyama, T.; Suzuki, R.; Takizawa, T.; Omata, D.; Maruyama, K.; Aramaki, Y. Delivery of siRNA into the cytoplasm by liposomal bubbles and ultrasound. *J. Controlled Release* **2008**, *132*, 124–130.

(33) Taniyama, Y.; Tachibana, K.; Hiraoka, K.; Aoki, M.; Yamamoto, S.; Matsumoto, K.; Nakamura, T.; Ogihara, T.; Kaneda, T.; Morishita, R. Development of safe and efficient novel nonviral gene transfer using ultrasound: enhancement of transfection efficiency of naked plasmid DNA in skeletal muscle. *Gene Ther.* **2002**, *9*, 372–380.

(34) Otani, K.; Yamahara, K.; Ohnishi, S.; Obata, H.; Kitamura, S.; Nagaya, N. Nonviral delivery of siRNA into mesenchymal stem cells by a combination of ultrasound and microbubbles. *J. Controlled Release* **2009**, *133*, 146–153.

(35) Shi, G.; Guo, W.; Stephenson, S. M.; Lee, R. J. Efficient intracellular drug and gene delivery using folate receptor-targeted pH-sensitive liposomes composed of cationic/anionic lipid combinations. *J. Controlled Release* **2002**, *80*, 309–319.

(36) Juffermans, L. J.; Dijkmans, P. A.; Musters, R. J.; Visser, C. A.; Kamp, O. Transient permeabilization of cell membranes by ultrasound-exposed microbubbles is related to formation of hydrogen peroxide. *Am. J. Physiol. Heart Circ. Physiol.* **2006**, *291*, H1595–H1601.

(37) Juffermans, L. J.; Kamp, O.; Dijkmans, P. A.; Visser, C. A.; Musters, R. J. Low-intensity ultrasound-exposed microbubbles provoke local hyperpolarization of the cell membrane via activation of BK(Ca) channels. *Ultrasound Med. Biol.* **2008**, *34*, 502–508.

(38) Zhou, Y.; Shi, J.; Cui, J.; Deng, C. X. Effects of extracellular calcium on cell membrane resealing in sonoporation. *J. Controlled Release* **2008**, *126*, 34–43.

(39) Kumon, R. E.; Aehle, M.; Sabens, D.; Parikh, P.; Han, Y. W.; Kourennyi, D.; Deng, C. X. Spatiotemporal effects of sonoporation measured by real-time calcium imaging. *Ultrasound Med. Biol.* **2009**, *35*, 494–506.

(40) Lelouvier, B.; Puertollano, R. Mucolipin-3 regulates luminal calcium, acidification, and membrane fusion in the endosomal pathway. *J. Biol. Chem.* **2011**, *286*, 9826–9832.

Pharm Res (2011) 28:712–719
DOI 10.1007/s11095-010-0286-4

RESEARCH PAPER

Delivery of an Angiogenic Gene into Ischemic Muscle by Novel Bubble Liposomes Followed by Ultrasound Exposure

Yoichi Negishi • Keiko Matsuo • Yoko Endo-Takahashi • Kentaro Suzuki • Yuuki Matsuki • Norio Takagi • Ryo Suzuki • Kazuo Maruyama • Yukihiko Aramaki

Received: 31 July 2010 / Accepted: 15 September 2010 / Published online: 8 October 2010

ABSTRACT

Purpose To develop a safe and efficient gene delivery system into skeletal muscle using the combination of Bubble liposomes (BL) and ultrasound (US) exposure, and to assess the feasibility and the effectiveness of BL for angiogenic gene delivery in clinical use.

Methods A solution of luciferase-expressing plasmid DNA (pDNA) and BL was injected into the tibialis (TA) muscle, and US was immediately applied to the injection site. The transfection efficiency was estimated by a luciferase assay. The ischemic hindlimb was also treated with BL and US-mediated intramuscular gene transfer of bFGF-expressing plasmid DNA. Capillary vessels were assessed using immunostaining. The blood flow was determined using a laser Doppler blood flow meter.

Results Highly efficient gene transfer could be achieved in the muscle transfected with BLs, and US mediated the gene transfer. Capillary vessels were enhanced in the treatment groups with this gene transfer method. The blood flow in the treated groups with this gene transfer method quickly recovered compared to other treatment groups (non-treated, bFGF alone, or bFGF+US).

Conclusion The gene transfer system into skeletal muscle using the combination of BL and US exposure could be an effective means for angiogenic gene therapy in limb ischemia.

KEY WORDS angiogenesis · bubble liposomes · gene delivery · ultrasound

INTRODUCTION

Skeletal muscle is a candidate target tissue for the gene therapy of both muscle (*e.g.*, Duschenne Muscular dystrophy) and non-muscle disorders (*e.g.*, cancer, ischemia, or arthritis). Its usefulness is due mainly to its stability and longevity after a gene transfer, which make it a good target tissue for gene therapy via the production of therapeutic proteins such as cytoskeletal proteins, trophic factors, or hormones. To achieve successful gene therapy in a clinical setting, it is critical that gene delivery systems be safe, easy to apply, and provide therapeutic transgene expression. Several previous studies using viral vectors reported the successful transfer of therapeutic genes into the target cells, but because of the considerable immunogenicity related to the use of viruses, non-viral gene transfer still needs to be developed (1). Recently, among physical non-viral gene transfer methods, it has been shown that therapeutic ultrasound enables genes to permeate cell membranes. The mechanism of gene transfer is believed to be involved in an acoustic cavitation (2–6). However, to achieve efficient gene transfer, a high

Yoichi Negishi and Keiko Matsuo have contributed equally to this work.

Y. Negishi (✉) · K. Matsuo · Y. Endo-Takahashi · K. Suzuki · Y. Matsuki · Y. Aramaki
Department of Drug and Gene Delivery Systems
School of Pharmacy, Tokyo University of Pharmacy and Life Sciences
1432-1 Horinouchi, Hachioji
Tokyo 192-0392, Japan
e-mail: negishi@toyaku.ac.jp

N. Takagi
Department of Molecular and Cellular Pharmacology
School of Pharmacy, Tokyo University of Pharmacy and Life Sciences
1432-1 Horinouchi, Hachioji
Tokyo 192-0392, Japan

R. Suzuki · K. Maruyama
Department of Pharmaceutics, Teikyo University
1091-1 Suwarashi, Midori-ku
Sagamihara, Kanagawa 252-5195, Japan

intensity of US is required, which leads to tissue damage (7,8). In contrast, low-intensity US in combination with microbubbles has recently acquired much attention as a safe method of gene delivery (9–13). However, microbubbles have problems with size, stability, and targeting function. Liposomes have been known as drug, antigen, and gene delivery carriers (14–18). To solve the above-mentioned issues of microbubbles, we previously developed the polyethyleneglycol (PEG)-modified liposomes entrapping echo-contrast, "bubble liposomes" (BL), which can function as a novel gene delivery tool by applying them with US exposure (19–24).

In the present study, we developed a safe and efficient gene delivery system into skeletal muscle using the combination of BL and US exposure. We assessed the feasibility and the effectiveness of BL for gene therapy by trying to deliver a bFGF-expressing plasmid into skeletal muscle in a hindlimb ischemia model through the combination of BL and US exposure.

MATERIALS AND METHODS

Materials

Preparation of Bubble Liposomes

Bubble liposomes were prepared by the previously described methods (19,22). Briefly, PEG liposomes composed of 1, 2-dipalmitoyl-*sn*-glycero-3-phosphocholine (DPPC) (NOF Corporation, Tokyo, Japan) and 1,2-distearoyl-*sn*-glycero-3-phosphatidyl-ethanolamine-polyethyleneglycol (DSPE-PEG_{2000}-OMe) (NOF corporation, Tokyo, Japan) in a molar ratio of 94:6 were prepared by a reverse phase evaporation method. In brief, all reagents were dissolved in 1:1 (v/v) chloroform/diisopropyl ether. Phosphate-buffered saline was added to the lipid solution, and the mixture was sonicated and then evaporated at 47°C. The organic solvent was completely removed, and the size of the liposomes was adjusted to less than 200 nm using extruding equipment and a sizing filter (pore size: 200 nm) (Nuclepore Track-Etch Membrane, Whatman plc, UK). The lipid concentration was measured using a Phospholipid C test Wako (Wako Pure Chemical Industries, Ltd., Osaka, Japan). BL were prepared from liposomes and perfluoropropane gas (Takachio Chemical Ind. Co. Ltd., Tokyo, Japan). First, 2-mL sterilized vials containing 0.8 mL of liposome suspension (lipid concentration: 1 mg/mL) were filled with perfluoropropane gas, capped, and then pressurized with a further 3 mL of perfluoropropane gas. The vial was placed in a bath-type sonicator (42 kHz, 100 W) (BRANSONIC 2510j-DTH, Branson Ultrasonics Co., Danbury, CT, USA) for 5 min to form BL.

Plasmid DNA (pDNA)

The plasmid pcDNA3-Luc, derived from pGL3-basic (Promega, Madison, WI), is an expression vector encoding the firefly luciferase gene under the control of a cytomegalovirus promoter. The plasmid pEGFP-N3 (Clontech Laboratories, Inc., Mountain View, CA) is an expression vector encoding the enhanced green fluorescein protein under the control of a cytomegalovirus promoter. The plasmid pBLAST-hbFGF (InvivoGen Inc.) is an expression vector encoding human bFGF under the control of an EF-1α promoter.

In Vivo Gene Delivery into the Skeletal Muscle of Mice with BL and US

ICR mice (5 weeks old, male) were anesthetized with pentobarbital throughout each procedure. A 40 μl suspension of pDNA (10 μg) and BL (30 μg) was injected into the tibialis (TA) muscle of the ICR mice, and US exposure (frequency: 1 MHz; duty: 50%; intensity: 2 W/cm^2; time: 60 s) was immediately applied at the injection site. A Sonitron 2000 (NEPA GENE, CO, LTD) was used as an ultrasound generator. Several days after the injection, the mice were euthanized and sacrificed, and the tibialis muscle in the US-exposed area was collected and homogenized. The cell lysate and tissue homogenates were prepared with a lysis buffer (0.1 M Tris-HCl (pH 7.8), 0.1% Triton X-100, and 2 mM EDTA). Luciferase activity was measured using a luciferase assay system (Promega, Madison, WI) and a luminometer (LB96V, Belthold Japan Co. Ltd., Tokyo, Japan). The activity is indicated as relative light units (RLU) per mg of protein. For analyzing EGFP expression, the treated muscle was fixed with paraformaldehyde and dehydrated in a sucrose solution. The specimens were embedded in an OCT compound and immediately frozen at −80°C. Serial sections 8 μm thick were cut by cryostat and observed with a fluorescence microscope (Axiovert 200 M, Carl Zeiss).

In Vivo Luciferase Imaging

The mice were anaesthetized and *i.p.* injected with D-luciferin (150 mg/kg) (Xenogen, Corporation, CA). After 10 min, luciferase expression was observed with an *in vivo* luciferase imaging system (IVIS) (Xenogen Corporation).

Tissue-Damage Testing Using Evans-Blue Dye (EBD)

Tissue-damage testing using EBD was performed as previously reported (25). Briefly, EBD was dissolved in PBS (10 mg/ml) and sterilized by using 0.2 μm membrane filters. Mice treated with pDNA, BL, and US exposure were administered with the dissolved EBD (0.5 mg dye per

10 g body weight) by tail vein injection. The mice were sacrificed 1 day after dye injection. The TA muscles were removed and photographed using a digital camera. The TA muscles were embedded in an OCT compound and immediately frozen at −80°C. Serial sections 10 μm thick were cut by cryostat and observed with a fluorescence microscope (Axiovert 200 M, Carl Zeiss).

Hindlimb Ischemia Model

The ischemic hindlimb model was created in five-week-old male ICR mice as previously reported (26). Briefly, animals were anesthetized, and a skin incision was made in the left hindlimb. After ligation of the proximal end of the femoral artery at the level of the inguinal ligament, the distal portion and all the side branches were dissected free and excised. The right hindlimb was kept intact to control the original blood flow. Immediately after ischemia was induced, a mixture of 40 μl of a pDNA (10 μg of pBLAST-hbFGF or pBLAST as an control vector) and BL (30 μg) suspension was injected into the adductor muscle of the ischemia mice, and US exposure (1 MHz, 2 w/cm^2, 50% duty cycle, 60 s) was immediately applied at the injection site. Measurements of the ischemic (left)/normal (right) limb blood flow ratio were performed for a set time using a laser Doppler blood flow meter (OMEGAFLO, FLO-C1).

bFGF ELISA

bFGF secretion was determined as previously reported (27). Briefly, 5- to 6-week-old male ICR mice were anesthetized by intraperitoneal injection of pentobarbital. The leg was shaved and depilated to expose the tibialis anterior muscle. Ten micrograms of DNA in a 40 μL bubble liposome or PBS solution were injected into the tibialis anterior muscle. After DNA injection, US exposure was applied. The tibialis anterior muscle was collected 2 days after the DNA injection. The muscle was washed three times in 3 mL of PBS to remove debris and blood. The washed muscle was placed in a 24-well plate coating growth factor reduced Matrigel (BD Biosciences) and incubated at 37°C. The muscle was grown in 1.5 mL of M199 medium containing 2% fetal bovine serum, 100 U/mL penicillin, and 100 mg/mL streptomycin. The levels of secreted cytokines in the conditioned media of the explants cultures were measured using human bFGF ELISA (R&D Systems), according to the manufacturer's instructions.

Immunohistochemistry

The ischemic thigh muscles were perfused on day 14 with PBS and 4% paraformaldehyde and embedded in paraffin. Muscle sections (4 μm) were stained with anti-CD31 antibody (BD pharmingen) overnight at 4°C. We then incubated the sections with Alexa Fluor 488 rabbit anti-rat IgG (Molecular Probes).

In Vivo Studies

Animal use and relevant experimental procedures were approved by the Tokyo University of Pharmacy and Life Science Committee and Teikyo University on the Care and Use of Laboratory Animals. All experimental protocols for animal studies were in accordance with the Principle of Laboratory Animal Care in Teikyo University.

Statistical Analyses

All data are shown as the mean±SD (n=4 or 6). Data were considered significant when $P<0.05$. The t-test was used to calculate statistical significance.

RESULTS

In Vivo Gene Delivery into the Skeletal Muscle of Mice with BL and US Exposure

It has been reported that microbubbles improve tissue permeability by cavitation upon US exposure. We first tried to deliver the naked pDNA (pCMV-Luc) into tibialis muscle using BL and US. A solution of pDNA and BL was injected into TA muscle, and US was immediately applied to the injection site, as shown in Fig. 1. As a result, the relative luciferase activity was high in the group treated using the pDNA plasmid with BL and US exposure. In contrast, there was low activity in the groups treated with pDNA alone, pDNA+BL, or pDNA+US. The luciferase activity in the group receiving a combination of BL with US exposure was 200- or 20-fold higher than that of the group treated with pDNA alone or pDNA + US, respectively (Fig. 1a). We next investigated whether their gene expression was derived from muscle cells. In a similar fashion, the EGFP expression plasmid (pEGFP-N3) was delivered into TA muscle, and 5 days after the gene delivery, the EGFP expression was sectioned and examined by fluorescent microscopy. As shown in Fig. 1b, the intramuscular gene delivery of the EGFP expression plasmid by BL and US exposure was present in a wide area of the positive muscle fibers of EGFP. In contrast, in the muscle specimens of the other treated groups (pDNA alone, pDNA+BL, or pDNA+US), very little expression was shown (Fig. 1b). We also observed the luciferase gene expression area in the whole body using an *in vivo* luciferase imaging system at 5 days after the transfection into the muscle treated with pDNA, BL, and US exposure.

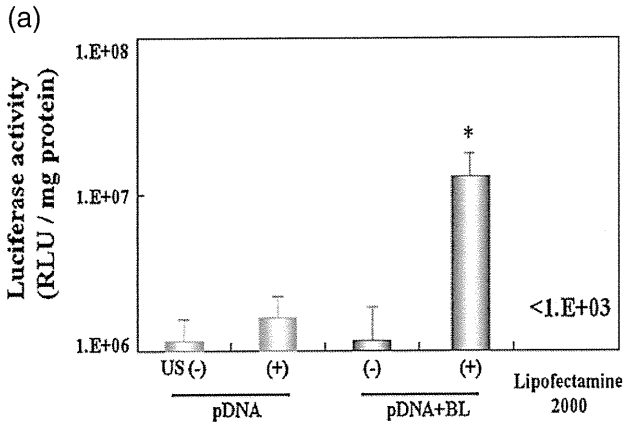

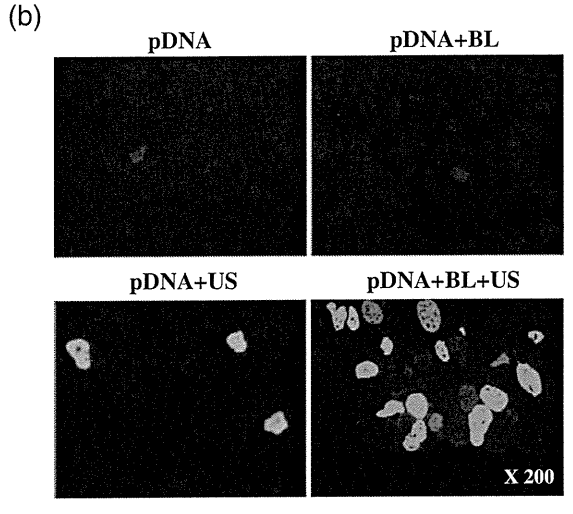

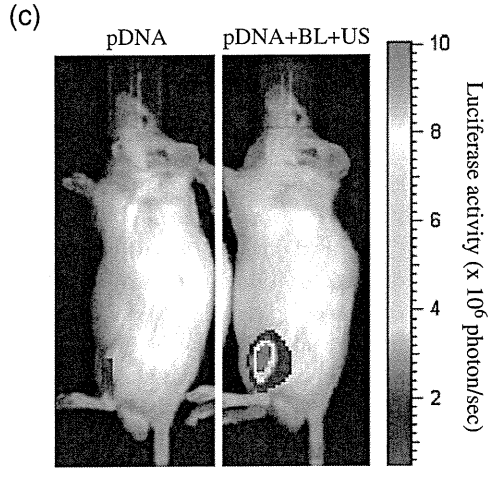

◀ **Fig. 1** Reporter gene expression after BL and US-mediated gene transfer compared with Lipofectamine 2000. (a) Luciferase expression after BL and US-mediated gene transfer compared with Lipofectamine 2000. Mice were treated with BL and US-mediated intramuscular luciferase gene transfer or Lipofectamine 2000. Five days after transfection, luciferase expression was determined. In another experiment, a pDNA (pCMV-Luc (10 μg))-Lipofectamine 2000 (25 μg) complex was suspended in PBS and injected into the left femoral artery. *$P < 0.01$ compared to the group of pDNA alone, pDNA + US, pDNA + BL, or Lipofectamine 2000 with BL. pDNA (pCMV-Luciferase): 10 μg, BL: 30 μg. US exposure (Frequency: 1 MHz, Duty: 50%, Intensity: 2 W/cm^2, Time: 60 s). (b) EGFP expression after BL and US-mediated gene transfer. Mice were treated with BL and US-mediated intramuscular EGFP gene transfer. Five days after transfection, EGFP expression was analyzed by fluorescent microscopy. Each of the gene transfer conditions are indicated above the pictures. Magnification: x 200. (c) photon counts are indicated by the pseudo-color scales.

Although the level of gene expression gradually decreased 2 weeks after the transfection using BL and US exposure, the moderate gene expression persisted for 4 weeks after the transfection (data not shown). The gene expression was restricted to the area of US exposure (Fig. 1c). This suggested that the combination of BL and US exposure facilitated the efficient transfection of pDNA into the muscle due to the induction of cavitation. We also assessed the tissue damage by testing EBD uptake in the muscle transfected with the BL and US exposure; however, significant tissue damage was not observed at the US condition (frequency: 1 MHz; duty: 50%; intensity: 2 W/cm^2; time: 60 s), even in the presence of the cavitation by BL and US exposure (Fig. 2b, e). When a higher US intensisty (4 W/cm^2) was applied, significant tissue damage was detected (Fig. 2c, f).

In Vivo Effects of the bFGF Expression System

We next attempted to deliver bFGF plasmid into tibialis muscle using BL and US and determine the bFGF protein expression in explant culture medium. The amount of bFGF protein was high in the group treated with bFGF plasmid with BL and US exposure. In contrast, there was low expression in the group treated with bFGF plasmid alone, or bFGF plasmid+US (Fig. 3). We further investigated the capillary density in order to know the effects of BL and US-mediated gene delivery with bFGF plasmid injected intramuscularly into hindlimb ischemia model mice. In the treatment group with BL and US-mediated gene transfer, their capillary vessels with CD31 positive cells were significantly increased compared to the treatment group of the control plasmid (empty vector), the bFGF plasmid alone, or bFGF plasmid + US (Fig. 4a, b). Measurements of the ischemic (left)/non-ischemic (right) hindlimb blood flow ratio were further performed for a period of time using a laser Doppler blood flow meter. Consistent with this induction of angiogenesis, the blood flow in the group treated with the bFGF plasmid with BL and US exposure was significantly increased compared with the group treated with the control plasmid (empty vector), the bFGF plasmid alone, bFGF plasmid + US (Fig. 5). Although we also examined the blood flow ratio after treatment with US exposure alone or BL with US exposure

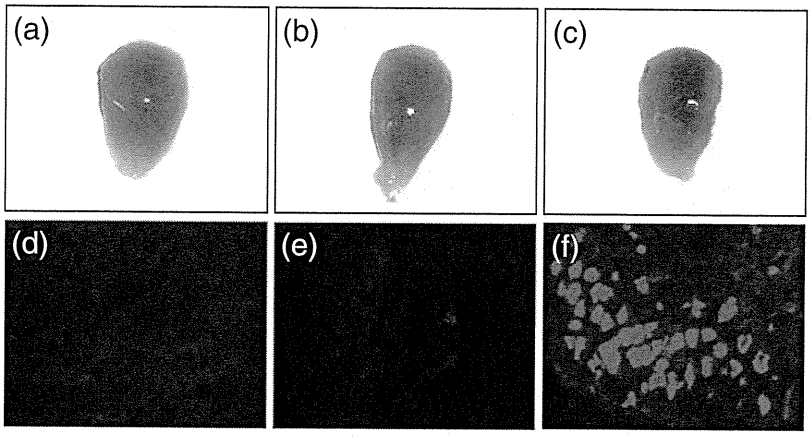

Fig. 2 Tissue-damage testing using EBD. pDNA alone without BL and US exposure (a, d). pDNA with BL and US exposure condition at a frequency of 1 MHz with an intensity of 2 W/cm^2 (b, e), or 4 W/cm^2 (c, f) for 60 s. The TA muscles were photographed using a digital camera (a, b, and c). Evans-blue fluorescence of 10 μm cryosections from the TA muscles was examined with fluorescence microscopy (d, e, and f). Magnification: ×100.

to the ischemic limb muscle, their blood flow ratio still remained in the 20 to 40% range. These results suggest that intramuscular injection of bFGF as an angiogenic gene with bubble liposomes followed by US exposure enabled us to improve an angiogenesis in the ischemic muscle.

DISCUSSION

The gene delivery of naked plasmid DNA is a feasible technique for non-viral gene therapy in a safe clinical use; however, a higher efficiency of site-specific delivery is required to achieve therapeutic effects in patients. In this view, we previously reported that BL is an efficient gene delivery tool (24,28,29). However, it is not enough to say that BL is a feasible and effective tool to carry out gene therapy to treat diseases. Here we demonstrate the development of a safe and efficient gene delivery system into skeletal muscle using the combination of BL and US exposure, and we assess the feasibility and the effectiveness of BL for angiogenic gene delivery. We therefore examined the potential ability of BL with US exposure to deliver a gene into skeletal muscle and its applicability for therapeutic angiogenesis in ischemic model. By using BL with US exposure, we first performed a transfer of luciferase-expressing plasmid DNA as a reporter plasmid into the TA muscle of mice. The remarkable gene expression could be enhanced efficiently only with the combination of both BL and US exposure when compared with other treatments (Fig. 1a). Exceeding our expectations, their gene expression was 200-fold higher than that of the plasmid DNA injection alone. When compared to Optison, one of the currently existing microbubbles (9–11), with US exposure, however, the gene transfer efficacy of BL was almost same as when using Optison (data not shown). Previously, our reports have demonstrated that the gene transfection efficiency *in vitro* could be affected with increasing the US intensity and the exposure time (20). The transfection efficiency increased with an increasing intensity of ultrasound and reached a plateau at 2 W/cm^2. No significant damage was observed under these conditions (Fig. 2b, e). When a higher intensity of US (4 W/cm^2) during the gene transfer with BL was applied to improve the transfection efficiency, the gene expression was conversely diminished (data not shown), and significant damage was also observed (Fig. 2c, f). This treatment caused significant tissue damage, probably due to the temperature elevation in the US exposure site. In this experiment, we therefore employed an US condition (frequency: 1 MHz; intensity: 2 W/cm^2; duty cycle: 50%; US exposure time: 1 min) that was in terms with a safety profile. As shown in Fig. 1b, the number of EGFP-positive muscle fibers could be apparently enhanced by the combination of BL and US

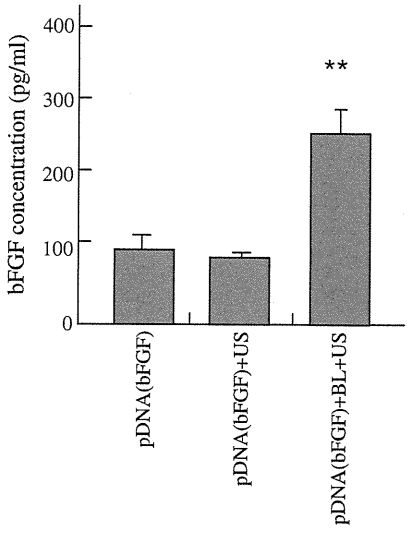

Fig. 3 bFGF protein expression after BL and US-mediated bFGF gene transfer. Mice were treated with BL and US-mediated intramuscular bFGF gene transfer. Two days after transfection, the muscle was collected and placed into Matrigel coating plates. After 3 days, the secreted bFGF protein expression was determined by ELISA. $^{**}P<0.05$ *vs.* other treatment groups. pDNA (pBLAST-bFGF): 10 μg, BL: 30 μg, US exposure (Frequency: 1 MHz, Duty: 50%, Intensity: 2 W/cm^2, Time: 60 s).

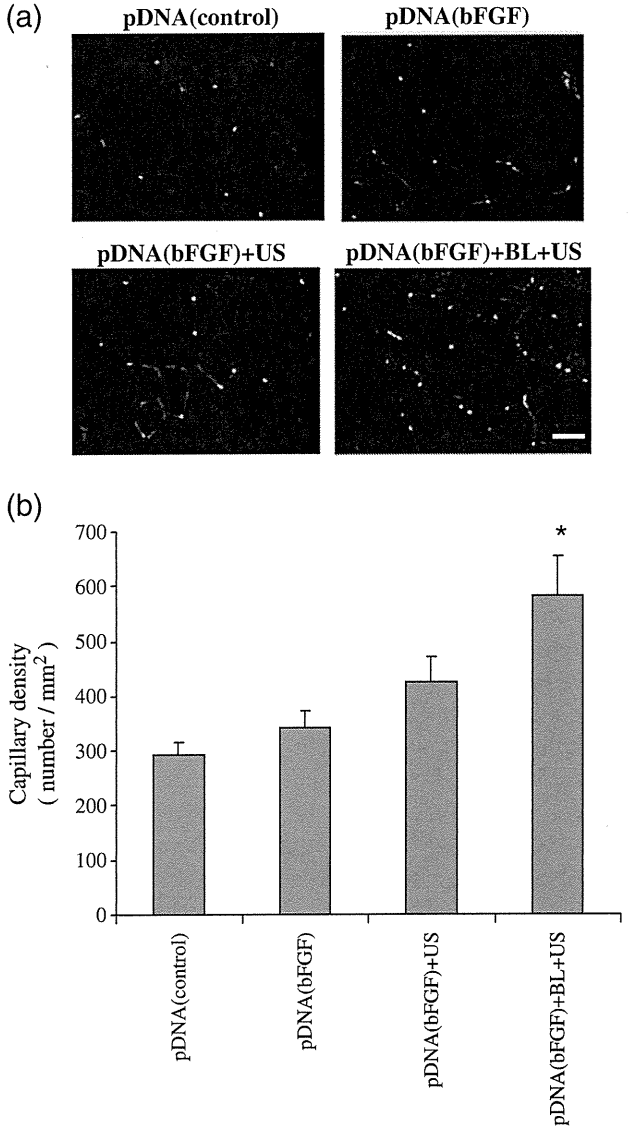

Fig. 4 Effect of BL and US-mediated bFGF gene transfer into hindlimb ischemia on capillary density. (a) CD31 staining of hindlimb muscle sections 14 days after BL and US-mediated bFGF gene transfer. The stained sections were analyzed by fluorescent microscopy. (b) CD31 positive vessels were measured. Green dots indicate CD31 positive vessels stained with an FITC-labeled anti-CD31 antibody. Scale bar represented 50 μm. *$P < 0.05$ *vs.* other treatment groups.

exposure; in contrast, without BL, only a few fibers could be observed in a treatment of US exposure without BL. Consequently, we found that a gene delivery method using BL and US exposure helped to both improve the transfection efficiency in the US focused site with a minimally invasive transfection procedure.

It is unclear whether BL with US exposure could improve transgene expression. Previously, we reported that BL could induce cavitation by a short duration (1–10 s) of US exposure and lead to efficient gene transfer into various types of cells (19,20). Therefore, the major biological effect of BL for gene delivery into the muscle may be through a cavitation induction, as was shown in previous reports (19). In contrast, in the case of Lipofectamine 2000, a commercial cationic lipid that is widely used in gene delivery, the transfection efficiency in the muscle was markedly lowered (Fig. 1a). This result is consistent with reports that serum proteins interact with and disturb cationic liposomes (29). It is expected that more time is required for this transfection, because cationic lipid/pDNA complexes (lipoplex) are entered into the cytoplasm by an endosomal pathway. Therefore, when the lipoplex with Lipofectamine 2000 was directly injected into the muscle, before it could enter into the cytoplasm by an endosomal pathway, it is possible that the degradation of pDNA or the aggregation of lipoplexes easily occurred. In contrast, once a solution of both BL and pDNA is administered into the muscle, US exposure is immediately applied at the injection site, leading to efficient gene expression, as shown in Fig. 1. In this way, unlike with lipoplexes, this simple method with BL and US exposure does not require a long time to achieve an efficient gene transfection. Our previous report has demonstrated that, by BL and US exposure, siRNA could directly enter into the cytoplasm without an endosomal pathway (22). In this report, because the level of gene expression corresponding

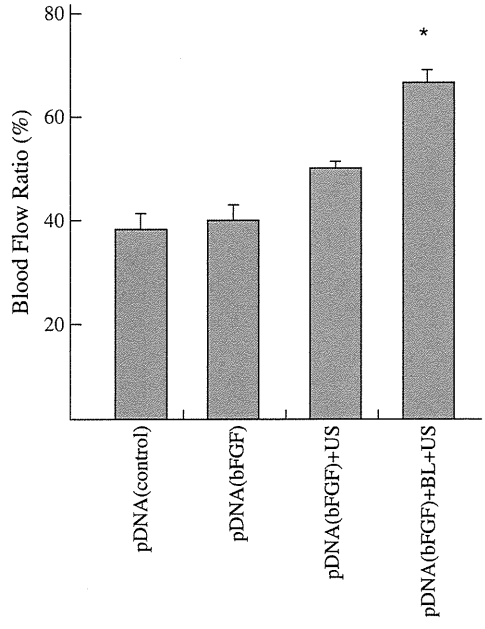

Fig. 5 Effect of BL and US-mediated bFGF gene transfer on the recovery of blood flow in ischemic limbs. After femoral artery ligation, mice were treated with BL and US-mediated intramuscular bFGF gene transfer. After the transfection, blood flow was measured at 14 days using a laser Doppler blood flow meter. *$P < 0.05$ *vs.* other treatment groups. Blood Flow Ratio (%): ischemic / normal blood flow ratio. pDNA (pBLAST-bFGF): 10 μg, BL: 30 μg, US exposure (Frequency: 1 MHz, Duty: 50%, Intensity: 2 W/cm^2, Time: 60 s).

to half of the expression in BL with a 1-minute US exposure could also be observed by BL with an only 10-second US exposure (data not shown), it may be thought that this transfection method by BL with US exposure enables immediate and direct pDNA delivery into the cytoplasm of muscle cells. The transfection efficiency might increase due to the appearance of transient holes in the cell membrane caused by the spreading of the BL, followed by their eruption with US exposure, which is consistent with previous reports using Optison (9).

Recently, a therapeutic strategy delivering angiogenic gene factors has been widely studied for clinical use in ischemic diseases (30). The delivery of naked plasmid DNA encoding an angiogenic gene into the ischemia has also been reported in clinical trials. However, the transfection efficiency is still insufficient for effective angiogenesis without side effects (30). Therefore, we assessed the feasibility and the effectiveness of BL for a gene therapy by trying to deliver a plasmid expressing bFGF, a key angiogenic factor, into the skeletal muscle of hindlimb ischemia model mice by the combination of BL and US exposure. As expected, with the gene delivery of the bFGF plasmid into an intramuscular injection with the combination of BL and US exposure, the capillary density and the blood flow ratio of the ischemic to non-ischemic hindlimb were markedly increased in the hindlimb transfected with the bFGF plasmid DNA through the combination of BL and a low intensity of US exposure compared to the plasmid DNA injection alone (Figs. 4 and 5). In addition, it has been reported that low-intensity US exposure can induce angiogenesis (31,32). However, no significant recovery in ischemic hindlimbs was observed with the combination of BL and US exposure without bFGF plasmid or with US exposure alone without the bFGF plasmid (data not shown). These results apparently indicate that therapeutic angiogenesis using naked plasmid DNA transfer that is enhanced by BL and US exposure could be a potential method in a clinical setting. We believe that there are several possibilities for BL usage in therapeutic angiogenesis with naked plasmid DNA in clinical use. The novel method using the combination of BL and US exposure may possibly reduce the amount of naked plasmid DNA, administration times, and the achievement of efficient gene transfer non-invasively without a viral vector, thereby enabling the decrease of the potential cost in clinical settings.

CONCLUSION

The present studies demonstrated a novel gene delivery method into skeletal muscle by the combination of BL and US exposure. Applied as gene therapy in a mouse model of ischemic limb muscle, intramuscular injection of bFGF as an angiogenic gene with BL followed by US exposure enabled improvement of an angiogenesis followed by apparent increased blood flow in the ischemic muscle. Because intramuscular injection of naked plasmid DNA alone may be inefficient and restrict its clinical use, this US-mediated BL technique may provide an effective non-invasive and non-viral method for angiogenic gene therapy for limb ischemia as well as for wound healing, ischemic heart disease, myocardial infarction, peripheral arterial diseases, and other various diseases.

ACKNOWLEDGEMENTS

We are grateful to Dr. Katsuro Tachibana (Department of Anatomy, School of Medicine, Fukuoka University) for technical advice regarding the induction of cavitation with US and to Mr. Yasuhiko Hayakawa, Mr. Takahiro Yamauchi, and Mr. Kosho Suzuki (NEPA GENE CO., LTD.) for technical advice regarding US exposure. This study was supported in part by the Industrial Technology Research Grant Program (04A05010) from New Energy, the Industrial Technology Development Organization (NEDO) of Japan, Grant-in-Aid for Scientific Research (B) (20300179) from the Japan Society of the Promotion of Science, and by a grant for private universities provided by the Promotion and Mutual Aid Corporation for Private Schools of Japan.

REFERENCES

1. Miller DG, Rutledge EA, Russell DW. Chromosomal effects of adeno-associated virus vector integration. Nat Genet. 2002;30:147–8.
2. Fechheimer M, Boylan JF, Parker S, Sisken JE, Patel GL, Zimmer SG. Transfection of mammalian cells with plasmid DNA by scrape loading and sonication loading. Proc Natl Acad Sci U S A. 1987;84:8463–7.
3. Miller MW, Miller DL, Brayman AA. A review of in vitro bioeffects of inertial ultrasonic cavitation from a mechanistic perspective. Ultrasound Med Biol. 1996;22:1131–54.
4. Joersbo M, Brunstedt J. Protein synthesis stimulated in sonicated sugar beet cells and protoplasts. Ultrasound Med Biol. 1990;16:719–24.
5. Greenleaf WG, Bolander ME, Sarkar G, Goldring MB, Greenleaf JF. Artificial cavitation nuclei significantly enhance acoustically induced cell transfection. Ultrasound Med Biol. 1998;24:587–95.
6. Schratzberger P, Krainin JG, Schratzberger G, Silver M, Ma H, Kearney M, *et al.* Transcutaneous ultrasound augments naked DNA transfection of skeletal muscle. Mol Ther. 2002;6:576–83.
7. Duvshani-Eshet M, Machluf M. Therapeutic ultrasound optimization for gene delivery: a key factor achieving nuclear DNA localization. J Control Release. 2005;108:513–28.
8. Kim HJ, Greenleaf JF, Kinnick RR, Bronk JT, Bolander ME. Ultrasound-mediated transfection of mammalian cells. Hum Gene Ther. 1996;7:1339–46.